AN ANALYSIS OF SOIL RESPIRATION IN A TEMPERATE DECIDUOUS FOREST ECOSYSTEM

By KATELYNN DALY, B.Sc.

A Thesis Submitted to the School of Graduate Studies in Partial Fulfillment of the Requirements for the Degree Master of Science

McMaster University

MASTER OF SCIENCE (2016)
(EARTH AND ENVIRONMENTAL SCIENCE)

McMASTER UNIVERSITY
HAMILTON, ONTARIO

TITLE: An Analysis of Soil Respiration in a Temperate Deciduous Forest Ecosystem

AUTHOR: Katelynn M. Daly, B.Sc. [Env. Chem.] (Thompson Rivers University)

SUPERVISOR: Dr. M. A. Arain

NUMBER OF PAGES: x, 65

ABSTRACT

The production and emission of carbon dioxide (CO_2) from soils, referred to as soil respiration (Rs), has a significant influence on the global carbon balance. Carbon is acquired by vegetation from the atmosphere through photosynthesis and stored on the surface and in soils as organic matter. This stored organic matter is returned to the atmosphere as CO_2 through belowground decomposition of organic matter by microbial communities (heterotrophic respiration) and metabolic activity of roots and mycorrhizae (autotrophic respiration). In this study, we explore temporal and spatial dynamics of Rs in a temperate deciduous forest located in Southern Ontario and how it is influenced by climatic controls over a two year period (2014/2015). The research site is a 90-year-old managed deciduous hardwood forest (Carolinian species) and part of the Turkey Point Flux Station and global Fluxnet network.

An automated soil CO_2 efflux system (LI-8100A) was utilized for continuous monitoring of Rs since July 2014 at our site. To better capture the spatial variability of Rs, a portable soil CO_2 efflux system (LI-6400) was also used along two 50-m transects. Comparing the two chamber systems, they both measured within one standard deviation of each other indicating that the long-term automatic chamber site is able to account for the spatial variability of the surrounding area. The coefficient of variation among automated chambers ranged from 15 to 85%.

The range of Rs measured during the two study years was 0.72 to 22.74 µmol CO_2 $m^{-2}s^{-1}$. Rs showed a strong soil temperature-driven seasonal trend, though soil moisture accounted for approximately 35% of the variability in Rs. Rainfall events were found to cause pulse response in Rs during and following the precipitation event, causing an 88% increase in Rs. Estimations of total CO_2 emissions at the site were modeled using four different techniques, and showed that Rs can account for approximately 84% of total ecosystem respiration. The average annual temperature sensitivity (Q_{10} value) of the study site was found to be 2.34. The annual Q_{10} model was improved by the incorporation of temporal variability of Rs (by estimating the Q_{10} model on a monthly basis) and also through the addition of a logistic soil moisture function. This study will allow us to have a better understanding of the dynamics of Rs and how it responds to its main controlling variables, soil moisture and temperature. It will also help us to determine the impact of climate change and extreme weather events on Rs in temperate deciduous forests and help in developing vegetation ecosystem models.

ACKNOWLEDGEMENTS

First and foremost, I would like to thank my supervisor, Dr. Altaf Arain, for providing me with the opportunity to pursue my Masters within his research group at McMaster University. Your endless support, advice and encouragement have been incredibly appreciated. I would also like to express my gratitude to my committee members, Dr. Sean Carey and Dr. Mike Waddington.

To the current and past members of the Hydrometeorology and Climatology Research Group, thank you so much for being a constant source of support and guidance. I wish to particularly thank Myroslava Khomik for her enthusiasm, dedication and wisdom. Thank you to Jason Brodeur and Hussein Wazneh for being an ever-helpful source of support with data processing. Rachel Skubel, Felix Chan, Jung Lee, Shawn McKenzie, Eric Beamesderfer, Brandon Burns, and Olivier Champagne, thank you for being incredible lab mates and friends, and for making this degree so enjoyable.

I am also thankful for the continuous support from my family, who have always encouraged and supported me throughout all my endeavors.

Funding was provided by the Natural Sciences and Engineering Research Council (NSERC), Ontario Ministry of Environment (OMOE), Canadian Foundation of Innovation (CFI), the Fluxnet-Canada Research Network , the Ontario Innovation Trust (OIT), and McMaster University. Support from Ontario Ministry of Natural Resources (OMNR), Natural Resources Canada (NRCan), Environment Canada (EC), the Canadian Carbon Program (CCP), the Canadian Forest Service (CFS) and the Long Point Recreation and Conservation Authority (LPRCA) are kindly acknowledged. I am also thankful to Jing Chen's research group (University of Toronto) for leaf area index measurements, Steve Williams and Ken Elliott (Ontario Ministry of Natural Resources), and Zoran Nesic from the Biometeorology and Soil Physics Group at the University of British Columbia for his continuous technical guidance.

TABLE OF CONTENTS

LIST OF FIGURES

Figure 8 The empirical relationship between soil respiration (Rs) in $\mu molCO_2m^{-2}s^{-1}$ and soil temperature (Ts) in ºC measured with the automated chamber temperature probes at 5cm depth during the two year (2014/2015) study period. The fitted Rs_Ts equations and R^2 were found to be $Rs=1.13e^{0.12Ts}$ and 0.63 for 2014 and $Rs=1.63e^{0.074Ts}$ and 0.37 for 2015.

Figure 9 Measured Rs values of daily mean soil respiration during the growing season (April- October) compared with predicted values using four models (Rs_Ts, Rs_Ts*SWC, Rs_Q_{10} and Rs_Q_{10}) in 2014 (a) and 2015 (b). Rs is recorded in $\mu mol\ CO_2\ m^{-2}s^{-1}$.

Figure 10 Observed soil respiration (Rs) plotted against modeled Rs and the coefficient of determination (R^2) for each of the four fitted models (Rs_Ts, Rs_Ts*SWC, Rs_Q_{10} and $Rs\_M\ Q_{10}$) for the growing seasons in 2014 (a, b, c, d) and 2015 (e, f, g, h). The numbers beside data points correspond to the month.

Figure 11 Taylor diagrams comparing model fits in terms of standard deviation, correlation coefficient and root mean square deviation (RMSD) in 2014 (a) and 2015 (b). The models are labelled as (A) Rs_Ts, (B) Rs_Ts*SWC, (C) Rs_Q_{10}, and (D) Rs_MQ_{10}.

Figure 12 A stacked bar plot showing the daily relative error of each of the four fitted models (Rs_ Ts, Rs_Ts*SWC, Rs_Q_{10} and $Rs\_M\ Q_{10}$) over the 2014 measurement period (Day of Year 190 to 339).

Figure 13 A stacked bar plot showing the daily relative error of each of the four fitted models (Rs_ Ts, Rs_Ts*SWC, Rs_Q_{10} and $Rs\_M\ Q_{10}$) over the 2015 measurement period (Day of Year 98 to 330).

Figure 14 The daily relative error of each of the four fitted models (Rs_Ts, Rs_Ts*SWC, Rs_Q_{10} and $Rs\_M\ Q_{10}$) plotted against temperature (ºC) for the growing seasons in 2014 (a, b, c, d) and 2015 (e, f, g, h). The numbers beside data points correspond to the month.

LIST OF TABLES

LIST OF ABBREVIATIONS AND SYMBOLS

TPFS	Turkey Point Flux Site
TPD	Turkey Point Deciduous research forest
FCRN	Fluxnet Canada Research Network
IPCC	International panel on climate change
C	Carbon
CO_2	Carbon dioxide
GPP	Gross primary productivity
RE	Ecosystem respiration
EC	Eddy covariance
Rs	Soil respiration
R_A	Autotrophic respiration
R_H	Heterotrophic respiration
SOM	Soil organic matter
Ta	Air temperature
PPT	Precipitation
Ts	Soil temperature
SM	Soil moisture content
LAI	Leaf area index
R_{10}	Basal rate of respiration at 10ºC
Q_{10}	Sensitivity of Rs to a temperature rise of 10ºC
Rs_Ts	Exponential Rs vs Ts model
Rs_Ts*SM	Q_{10} with a logistic SM function model
Rs_Q_{10}	Annual Q_{10} model
Rs_MQ_{10}	Monthly Q_{10} model
RMSD	Root mean square deviation
r	Coefficient of correlation
R^2	Coefficient of determination
RB	Relative bias
RE	Relative error
SD	Standard deviation
CV	Coefficient of variation

1. INTRODUCTION

1.1 Importance of forest ecosystems and the terrestrial carbon cycle

Forests account for 3.7 billion hectares of the planet's surface area, which is approximately 30% of the global land area (Schimel, 2014). They provide vital services at both global and regional scales; including the regulation of climate, hydrological cycles, air and water quality, and biogeochemical cycles (Apps & Price, 2013; Matsumono *et al.*, 2008). In addition to these ecosystem services, they are a significant economic resource as they support various industries related to lumber, pulp, and construction. Forests are also a major carbon pool, both above and below ground.

Carbon is the fundamental building block of all life on Earth, and an important component of many of Earth's physical processes. Terrestrial ecosystems play a central role in the global carbon cycle, with forests dominating the carbon exchange (Schimel, 2014). The major carbon influx occurs through the assimilation of atmospheric carbon dioxide (CO_2) from the atmosphere during photosynthesis by vegetation for the production of energy, which is stored within the carbon-carbon bonds of organic molecules. Some of these molecules are used as a source of energy through respiration, returning the carbon to the atmosphere as gaseous CO_2. The remaining carbon is temporarily stored within the vegetation biomass, and eventually enters the soil via litter fall from the aboveground biomass or as a result of relocation of biomass belowground for the construction and maintenance of roots (Brady & Weil, 2008; Lorenz & La, 2010). Forests are considered a natural climate regulator due to their ability to act as a major carbon reservoir (Apps & Price, 2013).

Without human interference the terrestrial carbon cycle is balanced, as evidenced by relatively small variations within the oscillations of historic CO_2 concentrations (Petit *et al.*, 1999; IPCC 2014). Since the Industrial Era, anthropogenic greenhouse gas emissions, particularly the burning of fossil fuels, is the primary cause of the observed unprecedented levels of atmospheric CO_2 concentrations (IPCC 2014). Changes in land use is the second largest source of anthropogenic CO_2 emissions, as deforestation has removed approximately half of the world's forests in response to increasing demand for timber and land for agriculture (Schimel, 2014). Upon conversion of forested land to agricultural land, 30% of stored forest soil carbon is released as CO_2 (Don *et al.*, 2011). Such conversions have led to 150-200 Pg of carbon lost to the atmosphere during the last two centuries (Don *et al*. 2013). This represents 20% of the total historical anthropogenic carbon emissions (Schimel, 2014).

In order to mitigate elevating CO_2 concentration, afforestation and other forest plantation and management strategies have been proposed as a potential means of carbon sequestration (Gonzalex-Beneck *et al.*, 2010). Terrestrial ecosystems hold a significant amount of carbon – approximately 500 Pg in aboveground vegetation biomass and 2000 Pg within the soil (Don *et al.*, 2013; Janzen, 2004). The ability of trees to absorb and store carbon over their long lifespan could enable them to be a valuable commodity in offsetting anthropogenic greenhouse gas emissions. Gross primary productivity (GPP) drives the sequestration of carbon in terrestrial ecosystems and subsequent production of biomass, producing biomass at a rate of approximately 90-100 Pg C annually on a global scale (Liao & Zhuang, 2015; IPCC 2014). Mitigation techniques would aim to increase global GPP and storage of carbon in biomass with long turnover times, such as wood or stable soil carbon pools (IPCC 2014). Consequently, great interest has emerged in understanding the role of terrestrial ecosystems, particularly forests, in the global carbon cycle and their potential in reducing the elevated atmospheric CO_2 concentrations.

1.2 Soil respiration

1.2.1 Soil respiration

Soils contain almost twice as much carbon as the vegetation and the atmosphere combined (Groenigen *et al.,* 2015), illustrating the importance of belowground carbon storage. Some studies have indicated that carbon acquired through photosynthesis is respired back to the atmosphere as gaseous CO_2 at an estimated global rate of 50-75 Pg of carbon per year (Lu *et al*. 2013). To put this into perspective, the soil carbon flux is approximately eleven times greater than the contribution of CO_2 to the atmosphere via fossil fuel combustion (Lu *et al*. 2013).

Soil carbon is returned to the atmosphere through the process of soil respiration (Rs) which refers to the total soil CO_2 efflux at the soil surface, expressed as µmol CO_2 $m^{-2}s^{-1}$. Soil respiration is comprised of belowground decomposition of organic matter as an energy source for microbial communities (heterotrophic respiration, R_H) and metabolic activity for maintenance and growth of plant roots (autotrophic respiration, R_A) (Savage *et al.*, 2013) (Figure 1). Quantifying Rs can indicate various physiological processes, as well as the ability of soil to support life including plants, animals, and microorganisms

(Lu *et al.*, 2013). Rs can describe the level of microbial activity, soil organic matter (SOM) content, and overall ecosystem metabolism (Ryan & Law 2005). Changes in Rs rates can also indicate external processes, such as disturbances (for example, cultivation) which typically increases Rs (Schlesinger & Andrews, 2000).

Studies have indicated that both R_A and R_H show similar seasonality, though R_A increases slightly later in the growing season than R_H (Hogberg *et al.*, 2001). The relative contributions of R_A and R_H reported in literature vary greatly, from 10% to 90%, depending on the type of ecosystem, the time of the year, and the measurement technique (Hanson *et al.*, 2000). Contributions of R_H to Rs have been reported as 66-82% of Rs in a 26-year old longleaf pine forest in western Georgia (ArchMiller & Samuelson, 2016), 52-56% in a boreal Scots pine forest in northern Sweden (Hogberg *et al.*, 2001), and 50% in a northern temperate deciduous forest in the Hudson Highlands, USA (Levy-Varon *et al.*, 2012).

1.2.2 Heterotrophic respiration

Heterotrophic respiration (R_H) involves the breakdown of organic molecules for energy by soil microorganisms. Plant-derived litter fall is the principal material that undergoes decomposition by heterotrophs, and can be classified into six groups with different rates of decomposition shown in Table 1. The decomposition process involves the oxidation of SOM to produce carbon dioxide, water, and energy (Equation 1), where energy is equivalent to 478 $kJmol^{-1}$ C:

$$\mathrm{OM} + 2\ \mathrm{O_2} \xrightarrow{Oxidation} \mathrm{CO_{2(g)}} + \mathrm{H_2O} + \mathrm{Energy} \qquad (1)$$

There are two categories of microbial decomposers involved in R_H: k-strategists and r-strategists (Brady & Weil, 2008; Thangarajan *et al*., 2013), and their activity throughout the growing season is dependent on the quantity and composition of the SOM (Figure 2). At the beginning of the growing season, little to no decomposable materials are being added to the soil via litter fall, resulting in low R_H rates. Microorganisms called *k-strategists* dominate R_H under these conditions, as they have developed enzymes with high affinity constants for resistant, stable organic substrates that take longer to decompose like cellulose and lignin. As the growing season continues and litter fall increases, more easily-decomposable plant materials such as sugars and proteins become available in the soil, resulting in an overall increase in microbial activity. The slower-acting k-strategists are out-competed by a group of organisms called *r-strategists*, which are classified by their rapid rates of growth and reproduction, resulting in a rapid increase in microbial biomass and CO_2 production (Fontaine *et al*., 2003; Brady & Weil, 2008). Towards the end of the growing season, the easily-decomposed compounds are depleted and r-strategist populations die or become dormant while k-strategists continue to survive (Fontaine *et al.*, 2003; Theenhaus & Scheu, 1996).

1.2.3 Autotrophic respiration

Autotrophic respiration (R_A) can be further broken down into that performed by roots and that by their associated mycorrhizae, which are fungi in a mutually beneficial association with plant roots (Figure 1). The fungal hyphae can grow 5 to 15 cm farther than the plant root, allowing the plant to increase its absorption surface area and subsequently increase its root system efficiency. This symbiotic relationship eliminates the need for mycorrhizae to compete with other soil heterotrophs for food sources, instead obtaining sugars directly from the plant's root cells (Brady & Weil, 2008). This relationship is particularly beneficial during drought conditions as large mycorrhizal communities facilitate increased capacity to take up water and nutrients, thus increasing drought survival rates of plants (Van der Molen *et al.*, 2011).

Though mycorrhizae fungi are technically heterotrophic root-associated soil microorganisms, during Rs studies they are generally considered part of R_A due to the methodological difficulty associated with differentiating between R_A and R_H during measurement (Tomè *et al.,* 2016).

1.3 Controlling factors on soil respiration

Rs is affected in a complex way by a number of factors. Soil temperature, soil water content and substrate supply are considered to be the most influential controls (Suseela *et al.*, 2012), particularly in temperate ecosystems (Ryan & Law, 2005). R_A and R_H are thought to respond differently to these controlling factors (Ma *et al*., 2014, Wei *et al.*, 2010).

1.3.1 Soil organic matter content

Soil respiration rates vary with different plant biomes, indicating that vegetation type has the ability to influence soil respiration because of the fact that vegetation directly determines soil microclimate and structure, as well as the quantity and quality of substrate supply (Raich & Tufekcioglu, 2000; Mitra *et al.*, 2014). SOM provides "food" or substrate for heterotrophic soil microbes and typically, assuming no other controls are limiting, adding SOM increases decomposition (R_H) and consequentially the overall Rs. Studies have shown that Rs increases nearly proportionally with the amount of readily degradable SOM (Raich & Tufekcioglu, 2000), with the exception of colder climates (such as boreal forests) due to colder temperatures which inhibit decomposition and result in accumulation of large amounts of SOM in soils (Schlesinger & Andrews, 2000).

1.3.2 Temperature

It is well known that temperature is a significant control on soil respiration, particularly on heterotrophic respiration (Suseela *et al.*, 2012). Rs increases exponentially as a function of temperature (Jia *et al.*, 2013), and is often modeled by a simple exponential function (Lloyd & Taylor, 1994; Khomik *et al.*, 2006) (Equation 2):

$$Rs = ae^{bTs} \qquad (2)$$

where Rs is the soil respiration (in $\mu molm^{-2}s^{-1}$), Ts is soil temperature (in ºC), and *a* and *b* are empirically derived coefficients. The sensitivity of Rs to Ts is typically expressed as the temperature coefficient (Q_{10} value) which is the factor by which respiration rate is changed by a temperature rise of 10°C. The Q_{10} model utilizes a modified version of the Van't Hoff equation (Van't Hoff, 1884) (Equation 3):

$$R_i = R_{10}\, Q_{10}^{\,(Ti - 10)/10} \qquad (3)$$

where R_i is the soil respiration measured at soil temperature T_i, and R_{10} (the basal Rs rate at 10ºC) and Q_{10} are parameters to be estimated. Q_{10} values reported in literature range from 1.3 to 8, varying both spatially and temporally (Jia *et al.,* 2013; Jacinthe & Lal, 2006). A general rule of thumb is that the typical Q_{10} for respiration in temperate forests is around two (Khomik et al., 2006; Davidson & Janssens, 2006; Noh et al., 2015), which means that the reaction rate will double for every 10° rise in temperature. Studies have indicated that the temperature sensitivity of soil respiration is inversely proportionate to temperature (Jacinthe & Lal, 2006). That is, at low temperatures soil respiration is very sensitive to temperature changes but this sensitivity decreases at high temperatures. The temperature sensitivity is often confounded by other additional drivers, such as soil moisture, microbial dynamics, photosynthetic processes and root activity (Jia *et al*., 2013; Wang *et al*., 2014; Han *et al*., 2014)

1.3.3 Soil moisture content

Soil moisture content (SM) is also a controlling factor on Rs due to its capacity to alter soil oxygen concentrations, which both R_H and R_A are sensitive to. An excess of water in soils will fill the soil pores and, in the absence of proper drainage, prevent the diffusion of oxygen into the soil from the atmosphere as the diffusion of gases is approximately 1,000 times slower in water than in air. This inhibits both aerobic root respiration and microbial decomposition (Brady & Weil, 2008). Low water content causes desiccation stress for autotrophic respiration and limitation of substrate diffusion for heterotrophic respiration (Van der Molen *et al*., 2011; Davidson & Janssens, 2006). Studies have shown that optimal conditions for Rs occur at intermediate water content (Davidson *et al.*, 1998).

High soil moisture can also alter the movement of CO_2 from its production sources in the soil to the atmosphere. An increased water content in pores acts as a barrier for diffusion as it greatly restricts the movement of gases in soils (Pumpanen *et al.*, 2008). High SM can also trigger an increase in Rs in the short term, for example after rain events pulse responses of Rs have been observed (Yan *et al.*, 2014; Gaumont-Guay *et al*., 2006).

1.4 Measurement techniques

Some of the earliest analyses of Rs were made nearly 90 years ago (Gainey, 1919). Original methods of measurements involved soil respiration chambers consisting of collars driven into the soil and covered with an enclosed chamber (called a 'respiration bell'), which measured increasing CO_2 concentrations using recordings of the absorption of CO_2 by a mixture of KOH and $Ba(OH)_2$ (Kutsch *et al*., 2010). Since then, methodology associated with Rs measurements have made significant advancements in chamber-based and partitioning methods.

Chamber-based methods are widely used in current soil respiration research (Khomik *et al*., 2006; Jia *et al*., 2013; Görres *et al*., 2015). There are two types of chamber methods to calculate soil CO_2 fluxes; (1) an open, steady state mode, where the difference in CO_2 concentrations is measured between the air flowing at a known rate through the inlet and outlet, or (2) a closed, non-steady state mode, where the chamber seals a known volume of air and the flux is calculated from the rate of increase of CO_2 over time (measured as the slope, through the use of infrared gas analyzers) (Ryan & Law, 2005; Kutsch, 2010).

There are three main problems associated with chamber-based soil respiration measurements: (1) altered soil climate and diffusion gradients, (2) disturbance to the soil structure, and (3) spatial variation concerns (Janssens *et al*., 2000; Davidson *et al*., 2002; Nagy *et al*., 2011). These errors can be avoided or minimized by implementing proper chamber designs that minimize disturbances to the soil profile and diffusion gradients (Görres *et al*., 2015), and spatial and temporal sampling regimes (Pavelka *et al*., 2007).

Field measurements of Rs are typically recorded as a combination of both R_A and R_H, since separating these two sources is challenging. One such partitioning method that has been successfully employed is root exclusion through trenching, where trenches are dug to sever existing roots to cut off the supply of photosynthates for R_A, theoretically allowing for the direct measurement of strictly R_H (Hanson *et al*., 2000; ArchMiller & Samuelson, 2016). Another common method is tree-girdling which involves stripping the stem bark of a tree in order to cut off its supply of photosynthates through the phloem to roots and mycorrhizae while still allowing water transport in the reverse direction through the xylem (Hogberg *et al*., 2001; Levy-Varin *et al*., 2012; Jing *et al*., 2015). Isotopic analysis the ^{13}C content of Rs to determine the age of carbon fixation can be used to partition the heterotrophic and autotrophic components, since R_H is fueled by soil carbon fixed months to years ago while R_A is fueled by carbon fixed hours or days ago through photosynthesis (Hogberg *et al*., 2008; Clemmensen *et al*., 2013; Snell *et al*., 2014).

During Rs measurements, respiration by heterotrophic root-associated microorganisms (such as mycorrhizae) is generally considered to be part of R_A due to the methodological difficulty associated with differentiating between them. Because of this, partitioning approaches such as tree girdling and trenching would potentially lead to an overestimation of R_A and an underestimation of R_H (Tomè *et al.*, 2016; Kuzyakov & Larionova, 2005). Even isotopic methods would not be able to distinguish between root and mycorrhizae respiration, as mycorrhizae receive a constant supply of photosynthates from roots (Van der Molen *et al*., 2011) so the ^{13}C signal from the heterotrophic fungi would indicate recent carbon fixation. Recent studies have shown success at addressing this problem using a modification of the trenching method, utilizing a mesh membrane to prevent roots from growing into a root-excluded plot while still allowing mycorrhizae to penetrate (Tomè *et al*., 2016; Moyano *et al*., 2008).

1.5 Significance of study

One of the main factors that make soil respiration a high interest topic is its sensitive relationship with future climate change. The current IPCC (2014) report estimates that global mean surface temperatures will rise by 3.7°-4.8°C in 2100 compared to pre-industrial levels with a range of 2.5°-7.8°C if efforts to reduce greenhouse gas emissions are not taken beyond what is in place today. Studies suggest that soil respiration will change with climate (Luo *et al.*, 2001; IPCC 2014), although the direction and extent of which this will occur is currently unclear. Predicted scenarios are difficult to confirm observationally due to the high spatial variability and difficulty measuring soil respiration on large scales (Bond-Lamberty *et al*., 2010).

The soil carbon reservoir is susceptible to increased rates of decomposition as temperatures increase (Savage *et al*., 2013; Tucker *et al.*, 2012), potentially increasing the average soil CO_2 flux to the atmosphere (Frey *et al*., 2012). A global temperature increase by 2°C is predicted to increase additional carbon release from soil by more than 10 Pg of carbon per year, increasing Rs carbon contributions by approximately 15-20% (Savage *et al*., 2012), which could in turn create a positive feedback cycle. Taking into account a coupled climate-carbon cycle model the mean surface temperature is predicted to rise by 8.0°C by the year 2100 (Luo *et al*., 2001), significantly higher than the current baseline IPCC estimate, illustrating the vast potential soils have to impact our climate.

Future climate change scenarios also involve an increase in extreme weather events, including more frequent precipitation (PPT) events (IPCC, 2014). It has been widely reported that soil respiration can increase significantly following a rainfall event (Lee *et al*., 2004; Yan *et al*., 2014). A better understanding of how a changing PPT regime could affect the rain pulse effect is important for predicting future Rs feedbacks to climate change.

Global Rs is typically modeled as a simple function of Ts, the Q_{10} function. However the response of Rs to Ts is confounded by multiple factors (Khomik et al., 2006; Jia et al., 2013). To improve the ability to model and predict future Rs, there is the need for a better understanding of how temporal, spatial, and environmental variations affect Rs. This understanding of Rs processes and the effect of its primary controls on its production, both spatially and temporally, is critical to evaluate the potential response of Rs to future climate change.

1.6 Research objectives

The objective of this study is to characterize the dynamics of Rs in a managed temperate deciduous forest located in Southern Ontario, Canada. This study is unique in that it utilizes both automated and manual soil CO_2 flux measurement systems. The automated chambers provide a temporally dense set, enabling a comprehensive visualization of daily and seasonal variations of Rs. This allows for more accurate and reliable empirical modeling and understanding of the effects of Ts and SM on Rs (Khomik *et al*., 2010; Koskinen *et al*., 2014), while manual chamber measurements provide a method of evaluating the spatial representativeness of the automated measurements (Savage & Davidson, 2003).

The specific objectives of this study are to (1) gain a better understanding of the spatial and temporal dynamics of Rs, (2) determine how Rs responds to its main controlling variables (i.e. soil temperature and soil moisture) and (3) help determine the impact of extreme weather events on Rs.

2. MATERIALS AND METHODS

2.1 Site description

This study was conducted in a 90-year old managed deciduous (Carolinian species) forest northwest of Long Point Provincial Park in Southern Ontario, Canada (42.64ºN, 80.56ºW). The forest is naturally regenerated on sandy terrain and abandoned agricultural land, and has been managed (thinned) in the past. The predominant tree species include: white oak (Quercus alba), sugar and red maple (Acer saccharu, A. rubrum), American beech (Facus grandifolia), black and red oak (Q. veluntina, Q. rubra) and white ash (Fraxinus americana). Average tree height is 25.7 m, with a stand density of 504 ± 18 trees per hectare. Average tree diameter at breast height is 22.3 cm. The leaf area index (LAI) of the site was measured by a plant canopy analyzer (model LAI2000, LI-COR, Lincoln, Nebraska, USA) and TRAC (Tracing Radiation and Architecture of Canopy, developed by Dr. Jing M. Chen’s group at the University of Toronto) as 8.0 m^2 m^{-2}. This site is part of the Turkey Point Flux Station (TPFS), and associated with Ameriflux and global Fluxnet Networks.

The topography is undulating, with well-drained, sandy soil (Brunisolic Gray Brown Luvisol) with low to moderate water holding capacity. The soil organic layer depth typically ranged from 2 to 6 cm. In September of 2014, soil cores and litter samples were taken and sent for nutrient analysis (A & L Canada Laboratories, Inc., London, Ontario). The samples were analyzed for total organic matter content, carbon, nitrogen, phosphorous, potassium, magnesium, calcium, and other additional soil characteristics. The soil nutrient content is outlined in Table 2. 30-year climate normals, based on 1981-

2010 Environment Canada weather data collected at Delhi, Ontario CDA weather station, indicate a mean annual air temperature (Ta) of 8.0ºC and mean annual precipitation (PPT) of 1036 mm (906.4 mm of which falls as rain and 129.5 cm as snow).

2.2 Soil respiration measurements

Continuous Rs was recorded using an automated soil CO_2 flux measurement system, taking half hourly measurements from July 2014 to November 2015 (excluding winter months). It was comprised of three main components: the gas analyzer (hosted in an analyzer control unit) (LI-8100A), long-term measurement chambers (LI8100-104), and a multiplexer to allow for multiple chamber measurements (LI-8150) (LI-COR Lincoln, Nebraska, USA). Two measurement chambers were employed from July to December 2014, and increased to five from April to November 2015. Each chamber extended approximately 15 m from the central analyzer control unit and multiplexer, measuring half-hourly Rs in sequence. Chambers were equipped with a soil temperature (Ts) and soil moisture (SM) probe at 5 cm depth installed outside of the collar.

The soil collars used are comprised of thick-walled PVC pipe with an internal diameter of approximately 20 cm, a height of 11.5 cm, and a thickness of 1 cm. Each collar was inserted approximately 7-8 cm into the soil surface, with 3 cm remaining above. The measurement chamber was placed directly on the soil collar, remaining open when not taking active measurements. Throughout the growing season, any vegetation growth was removed from inside the collars to eliminate potential photosynthesis effects.

Manual measurements of Rs were measured on a bi-weekly to monthly basis using a LI-COR LI-6400 portable photosynthesis system with a LI-6400-09 soil chamber attachment (LI-COR Lincoln, Nebraska, USA). Measurements were taken along two 50 m transects, each containing 10 permanent sampling locations. Soil collars were made of PVC pipe, with an internal diameter of approximately 10 cm and height of 7.5 cm. Each collar was inserted into the soil to approximately 5 cm depth. At each sampling point, three replicate Rs measurements were recorded along with Ts and SM. Both automatic and manual soil CO_2 chambers systems used in this study are infrared gas analyzer (IRGA)-based systems, operating as a closed, non-steady state system.

2.3 Eddy Covariance Flux and Meteorological measurements

Ecosystem CO_2 fluxes (ecosystem respiration, RE) were measured using closed-path eddy covariance system, comprising of a sonic anemometer (CSAT3, Campbell Scientific Inc. (CSI), Edmonton, AL, Canada) and infrared gas analyzer (LI-7200, LI-COR Inc., Lincoln, NE, USA) as well as meteorological measurements using an automatic weather station (CSI). Flux and meteorological instruments were installed above the canopy at about 36 m height on top of a walk-up scaffolding tower. A mid-canopy infrared gas analyzer, IRGA (model LI-820, LI-COR) was used to measures mid-canopy CO_2 concentration at 16 m above ground, which was used to estimate CO_2 storage within the forest air column. Ts and SM were measured year-round at two locations at multiple depths (2, 5, 10, 20, 50, 100 cm) alongside the eddy covariance flux near the tower and soil CO_2 chambers locations. Eddy covariance flux measurements were made at 20 Hz and saved as half hourly data. Meteorological and soil data were sampled at 5 second intervals and averaged to half hourly data using a data logger (model CR3000, CSI). Eddy covariance flux, soil chamber CO_2 flux and meteorological measurements have been continue at this site, however measurements made after December 31, 2015 are not included in this analysis.

2.4 Data analysis

Linear and exponential regression analyses were performed on daily means of measured Rs data for gap filling. Four simple, empirically driven models were derived to determine the correlation between Rs and its main environmental controls (Ts and SM), outlined in Table 5. The first was a simple, exponential regression between Rs and Ts (Rs_Ts, Equation 2), and the remaining models were versions of the Q_{10} model (Equation 3). An annual Q_{10} was fit for each year (Rs_Q_{10}), and the Q_{10} model was modified with a logistic SM function (Peichl *et al.*, 2010) to incorporate soil moisture effects (Rs_Ts*SM):

$$\mathrm{Rs} = \mathrm{R}_{10}\times\mathrm{Q}_{10}^{((\mathrm{Ts}-10)/10)}\times\left(\frac{1}{1+e^{a+b*SM}}\right) \qquad (4)$$

where Rs is predicted soil respiration (in µmol CO_2 $m^{-2}s^{-1}$), Ts is soil temperature (in ºC), SM is soil moisture (in $m^3m\text{-}^3$), and R_{10}, Q_{10}, *a* and *b* are fitted temperature coefficients. The fourth model was a Q_{10} model fit on a monthly basis (Rs_MQ_{10}) outlined in Table 6.

Modeled daily Rs was calculated from continuous Ts and SM data available from the weather station and the automated soil CO_2 chamber measurement system. Daily mean Ts and SM values (measured at 5cm depth) were used as input to the models. Each model was used to simulate daily, seasonal (spring = April - May, summer = June - August, Autumn = September - October) and growing season (April - October) Rs emissions, and compared to ecosystem respiration data derived from eddy covariance measurements. Calculated daily Rs emissions were converted to grams of C per meter squared per day and summed to seasonal and growing season sums.

Root mean square deviation (RMSD), coefficient of correlation (r), coefficient of determination (R^2), relative bias (RB) and relative error (RE) were used to evaluate model performance. The range, standard deviation (SD), and coefficient of variation (CV) were taken as indicators of the degree of spatial variability in Rs.

3. RESULTS

3.1 Meteorological measurements

The annual course and monthly average values of selected meteorological and soil variables during the study period are shown in Figure 3 and Table 3. Monthly average air temperature (Ta, Figure 3a) ranged from -7.6 and -6.2 ºC in the winter seasons to 20.1 and 21.3 ºC in the summer seasons in 2014 and 2015, respectively. The mean annual Ta values were 7.9 and 9.0 ºC in 2014 and 2015, respectively. The 30-year mean Ta value is 8.0ºC in the region (Environment Canada, Delhi Station). In April Ta rose above 0 ºC, continued to rise until August after which Ta gradually declined for the rest of the year.

The seasonality of photosynthetically active radiation (PAR, Figure 3a) and soil temperature (Ts, Figure 3b) followed closely that of Ta, with the exception of the late winter (January to March) where Ts remained consistently near 0 ºC. Monthly average Ts values ranged from -0.05 and -0.04 to 17.8 ºC and 18.1 ºC in 2014 and 2015, respectively. Maximum values for incoming photosynthetically active radiation (PAR, Figure 3a), Ta and Ts occurred in the summer months. In 2014 PAR reached maximum values in June, coinciding with maximum Ta values, whereas in 2015 maximum PAR and Ta were reached in July.

Total annual precipitation (PPT) (Figure 3c) at the site was 1430 and 810 mm in 2014 and 2015, respectively. The regional 30-year mean value of the area is 1036 mm (Environment Canada, Delhi Station). The site received approximately 703 and 576 mm of precipitation throughout the growing season (April through October) of 2014 and 2015, respectively.

Soil moisture content (SM), shown in Figure 4, peaked in early spring with maximum values of 0.23 and 0.19 m^3m^{-3} in April of both 2014 and 2015, respectively. SM decreased during the summer months, reaching minimum values of 0.032 and 0.027 m^3m^{-3} in July 2014 and September 2015, respectively. There was a second SM peak in late autumn, reaching 0.15 m^3m^{-3} in October of 2014 and 0.11 m^3m^{-3} in November of 2015. Average SM values were found to be 0.12 m^3m^{-3} in 2014 and 0.09 m^3m^{-3} in 2015.

3.2 Seasonal and annual trends in Rs

The daily Rs recorded by automated and manual chamber measurements during the study period are shown in Figure 5. The seasonal trend of Rs followed closely that of Ta and Ts, reaching its maximum values in the summer months, then followed a declining trend throughout the rest of the year. Maximum daily mean Rs of 12.09 and 11.66 µmol CO_2 $m^{-2}s^{-1}$ were recorded on August 5th 2014 and June 14th 2015, respectively, while daily minimum mean Rs of 0.72 and 1.37 µmol CO_2 $m^{-2}s^{-1}$ were recorded on December 11th 2014 and November 20th 2015, respectively.

An increase in Rs rates during and following precipitation events was observed. For example, on September 2nd, 2014 there was a 22.4 mm precipitation event which caused an increase of SM of 0.1 to 0.28 m^3m^{-3} and an 88% increase in Rs from 6.5 to 12.2 µmol CO_2 $m^{-2}s^{-1}$ (Figure 6). Rs did not return to pre-rain event Rs until September 8th, 6 days after the rain event.

Measured growing season (April-October) Rs was found to be 800 and 976 g C m^{-2} in 2014 and 2015, respectively. Growing season totals may be underestimated as percentages of missing data amounted to 46.3% of 2014 and 17.9% of 2015 (Table 4). Maximum Rs rates and carbon loss were measured in the summer months (June-August), contributing 484 and 621 g C m^{-2} in 2014 and 2015, respectively.

3.3 Spatial variability

The coefficient of variation (CV) among automated measurement chambers in 2015 varied between 15 to 85% and averaging 50% (n=5).

In order to assess the ability of the automated chambers to account for spatial variability in Rs, manual chamber measurements were taken along two additional transects periodically and compared to the automated chamber measurements made within the same time frame. The automated and manual chambers showed good agreement throughout the majority of the study period (Figure 7). The automated chamber measurements measured within 1 standard deviation of both manual chamber measurements along Transect 1 (T1) and Transect 2 (T2) 93% of the time.

T1, which ran alongside the automated chamber measurement site, had a mean SM value of 0.12 m^3m^{-3} and mean Ts of 15.2 ºC. T2 had a similar mean Ts of 14.8ºC, but a higher mean SM of 0.16 m^3m^{-3}. Rs measured at T1 was most similar to the automated chamber measurements, with a range of 1.01 – 8.91 μmol CO_2 $m^{-2}s^{-1}$ and a mean of 5.01 μmol CO_2 $m^{-2}s^{-1}$. Rs measurements with the automated chambers ranged from 1.28 – 10.0 μmol CO_2 $m^{-2}s^{-1}$, averaging 5.14 μmol CO_2 $m^{-2}s^{-1}$, while T2 ranged from 1.08 – 5.0 μmol CO_2 $m^{-2}s^{-1}$, averaging 3.0 μmol CO_2 $m^{-2}s^{-1}$.

3.4 Controlling factors on Rs

Rs displayed a strong, positive, exponential relationship with Ts in both years of the study period (Figure 8). Further analysis of the temperature relationship found that the annual temperature sensitivity (Q_{10} values) in 2014 and 2015 were 3.92 and 1.65, respectively. The difference in Q_{10} values between these two years could be due to the high percentage (46%) of missing data in 2014, failing to take into account the early growing season Rs trends. Incorporating both 2014 and 2015 data sets, the site Q_{10} was found to be 2.34.

This study found that the temperature sensitivity of soil respiration varied temporally. A single Q_{10} and R_{10} coefficient was calculated for each month during active measurements, outlined in Table 5b. The Q_{10} of Rs decreases with increasing Ts values, while R_{10} values increase. The lowest R_{10} values (2.07 to 3.30 μmol CO_2 $m^{-2}s^{-1}$) occur during early and late growing season when monthly average Ts was approximately 12ºC. The highest R_{10} (8.33 μmol CO_2 $m^{-2}s^{-1}$) and lowest Q_{10} (0.86) occurred when Ts was equal to or greater than 18ºC, corresponding to the summer months of 2015. The highest Q_{10} value (4.97) was observed in early summer when Ts was below 15ºC.

Even between months with identical monthly mean Ts values, there were seasonal differences in R_{10} and Q_{10}. For example, in both May and October of 2015 the monthly mean Ts was approximately 12 ºC. However the Q_{10} and R_{10} were lower in May (2.26 and 2.07 μmol CO_2 $m^{-2}s^{-1}$, respectively) than in October (2.89 and 3.30 μmol CO_2 $m^{-2}s^{-1}$, respectively).

There is a statistical difference between Q_{10} values calculated between years. For example, Q_{10} was found to be 2.93±0.05 in September of 2014, but 1.11±0.08 in September of 2015. This could be reflective of differences in climatic and soil conditions. In September, monthly PPT was 129% higher and SM was 120% higher in 2014 than 2015, which indicates that SM may have contributed to these differences.

3.5 Comparison of Rs models

Four models were fit to measured Rs data from 2014 and 2015 data for the purpose of comparing model fits. Three were annual models (parameters outlined in Table 5a) and one was fit on a monthly basis (parameters outlined in Table 5b). A comparison of modeled and observed daily mean Rs during the growing season of both years are shown in Figures 9. The modeled vs observed Rs regression analysis and the coefficient of determination (R2) for each model is shown in Figure 10. The regression lines are much closer to the 1 1 line and the R2 shows improvement with the Rs_Ts*SM model (Figure 10, b and f) and Rs_MQ10 model (Figure 10, d and h).

Taylor diagrams, comparing the models in terms of standard deviation, correlation coefficient, root mean square deviation (RMSD), are displayed in Figure 11. In 2014, the model that best fit the data was found to be the monthly Rs_MQ$_{10}$ (model D in Figure 11) as it is highly correlated with measured values (producing a correlation coefficient of 0.9), and had the lowest RMSD value (1.17). However the Rs_MQ$_{10}$ model had a lower standard deviation (2) than the measured Rs (2.46), indicating it would not be able to reproduce the seasonal variability of the Rs data. The Rs_Ts*SWC model (model B in Figure 11) fitted to measured half-hourly Rs data achieved a high correlation coefficient and a low RMSD value, but had the furthest standard deviation from the measured data. The Rs_Ts (model A) and Rs_Q$_{10}$ models (model C) fitted to measured half-hourly Rs data reproduced the variability of the data as they had the closest standard deviation to the measured values, but they did not achieve as desirable of a correlation coefficient or RMSD value as model B and D.

In 2015, when more complete measured Rs data was available, the Rs_MQ$_{10}$ model showed the best fit, with a correlation coefficient of 0.87 and RMSD value of 1. It also had a standard deviation of 1.96, very close to the standard deviation of the measured data set (2.1). The Rs_Ts*SM model had the next best fit with a correlation coefficient of

0.77, an RMSD value of 1.41, and a standard deviation of 2.1. The remaining two models were not well correlated, all producing correlation coefficients of approximately 0.6, and RMSD values greater than 1.5.

A further statistical analysis of each model is outlined in Table 6. Overall the Rs_M$_{10}$ and Rs_Ts*SM models had the best fit, explaining an average of 77 and 65% of the variability in the observed Rs data. The effect of SM was able to be examined through the comparison of the conventional Q$_{10}$ model (Rs_Q$_{10}$) and the Q$_{10}$ model with the addition of a logistic SM function (Rs_Ts*SM). The Rs_Q$_{10}$ model obtained an R^2 of 0.20 in 2015, while the Rs_Ts*SM model obtained an R^2 of 0.55. This indicates that SM accounted for 35% of the variability in the data. In 2014 the difference in R^2 was 0.05, which could be due to fact that only the second half of the growing season was measured in 2014.

To better visualize the temporal trends in model fit, the daily relative error of each of the fitted models were plotted in a stacked bar plot over both the 2014 (Figure 12) and 2015 (Figure 13) study period. There were clear seasonal trends in the estimation of all models. In both years they were producing positive relative error values during the summer months (June, July and August), representing an underestimation of Rs. Towards the end of August until the end of the measurement period the models were producing negative relative error, indicating an overestimation of Rs. There were large relative error values of the models in the spring of 2015. This could be the result of instrumentation problems causing a loss of 57% of spring Rs data in 2015, inhibiting the ability to produce a model that accurately predicts Rs during that season. Both Figure 12 and Figure 13 indicate that the Rs_MQ_{10} and Rs_Ts*SM models have the lowest relative error of the four models.

The daily relative error of each of the fitted models was plotted as a function of temperature in Figure 14. The Rs_MQ_{10} model (Figure 14,d & h) show the most uniform relative errors across all measured Ts ranges (2 to 22ºC). The Rs_Ts (Figure 14,a & e) and Rs_Q_{10} models (Figure 14,c & g) produced positive relative error values in the summer months and negative relative error in the autumn. The Rs_T_s*SWC (Figure,14 b & f) model showed largely negative relative error at lower Ts and positive relative error at higher Ts.

All models showed positive relative error in April and negative error in May. Due to loss of a large percentage of spring measured data, the time period when recorded soil temperatures were within the 2 to 8ºC range, the ability of our model to represent spring Rs was likely reduced.

Each model was used to simulate seasonal and growing season Rs emissions, which are summarized in Table 7. Across all four models, spring had the lowest estimated carbon emissions (156 to 231 g C m^{-2} in 2014 and 150 to 195 g C m^{-2} in 2015). The highest estimates were in the summer season (587 to 925 g C m^{-2} in 2014 and 468 to 628 g C m^{-2} in 2015), with emissions declining again in the autumn (321 to 437 g C m^{-2} in 2014 and 267 to 325 g C m^{-2} in 2015). Measured growing season ecosystem respiration (RE) was 935 ± 2.3 g C m^{-2} in 2014 and 1049 ± 3 g C m^{-2} in 2015. No model estimated below 1100 g C m^{-2} in 2014. The lowest carbon emissions estimated in 2015 was by the Rs_MQ$_{10}$ model, estimating 885±2.2 g C m^{-2}.

4. DISCUSSION

4.1 Temporal patterns of Rs

Significant seasonal variation of Rs was observed at our site. Rs increased in spring and then peaked in summer, coinciding with maximum PAR, Ta and Ts, which provided optimal conditions for high rates of photosynthesis and respiration. Rs then declined into autumn, following the seasonal dynamics of Ts rather than SM. This indicates that Ts was the main driver of temporal variation in Rs, which is comparable to the results of Rs measured in other temperate forests (Taylor *et al*., 2015; Shabaga *et al*., 2015).

The effect of temperature on Rs can be expressed using the Q$_{10}$ model coefficients, R$_{10}$ and Q$_{10}$ (Equation 3). The basal respiration rate at 10ºC (R$_{10}$) is related to the volume of the soil column that is biologically active, i.e. the size and activity of the microbial and root population (Mo *et al*., 2005). The Q$_{10}$ value is the temperature sensitivity of Rs to warming (Jia *et al*., 2013). The Q$_{10}$ and R$_{10}$ values obtained at our site were found to be 1.11 to 8.33, within the range of literature-reported values (Jacinthe & Lal, 2006; Khomik *et al*., 2006; Noh *et al*., 2015), and followed distinct seasonal trends. It was found that R$_{10}$ values increase with increasing T$_s$ values, while Q$_{10}$ values decrease, which is consistent with many previous studies (Janssens *et al*., 2004; Gaumont-Guay *et al*., 2006; Jia *et al*., 2013). The higher Q$_{10}$ at lower Ts can be explained by the higher sensitivity of soil microbial populations (R$_H$) to temperature fluctuations at low Ts (Mo *et al*., 2005). It is also related to plant phenology as it can reflect changes in root activity and associated respiration (Jia *et al*., 2013). The main driver of R_A is substrate provision through photosynthesis, but sensitivity to temperature can be the result of environmental factors that co-vary with temperature, such as light-dependent production of photosynthates and changes in root biomass (Hogberg *et al*., 2001; Mo *et al*., 2005; Wei *et al*., 2010).

There were seasonal differences in R_{10} and Q_{10} at our site, even between months with similar mean Ts, as expected. For example, May and October of 2015 had identical mean Ts (12ºC) but the R_{10} and Q_{10} values were lower in May. Studies in literature have found that regardless of identical Ts, higher R_{10} values are reported in the autumn months due to the larger active volume of the soil as a result of the warming of deeper soil layers during the summer and accumulation of fresh litter (leading to higher levels of microbial activity) compared to spring (Jia *et al*., 2013; Mo *et al*., 2005).

Seasonal variations in Rs can be largely accounted for by variations in Ts, but there are inconsistencies in the temperature effect that can be explained by other environmental controls such as soil moisture as mentioned earlier and in many studies in literature. (Davidson *et al*., 1998; Xu & Qi, 2001; Pumpanen *et al*., 2008; Van der Molen *et al*., 2011). One example of this is increases in Rs after high levels of precipitation at our site. We observed pulse responses of Rs following large rainfall events (Figure 6), which is consistent with results reported in a number of field studies (Lee *et al.*, 2004; Gaumont-Guay *et al*., 2006; Yan *et al*, 2014). This is mainly attributed to an increase in decomposition by soil microbial communities (Lee *et al*., 2002; Gaumont-Guay *et al*., 2006). Following a rain event, CO_2 in soil pore spaces is replaced with rainwater, causing a surge in CO_2 efflux at the soil surface, and microbial populations and activity increase to decompose carbon compounds within the litter and upper soil layers (Yan *et al*., 2014).

Few studies have quantified the total contributions of Rs pulses following rain events to total Rs. Lee *et al* (2002) reported an increase of Rs rates of 16-21% following rain events in a temperate deciduous forest in Japan. Liu *et al* (2015) conducted a meta-analysis on precipitation treatments across multiple biomes and found that precipitation events in temperate forests cause an increase in Rs of 17-30%. Our site experienced pronounced increases in Rs after precipitation events, larger than those typically reported for temperate deciduous forests in literature, which could be the result of the well-drained, sandy soils and climatic conditions at our site, which receives half the amount of precipitation than the site studied by Lee *et al* (2002). We suggest that the relatively low SM (0.03 to 0.23 m^3m^{-3}) and good drainage could result in a rainfall pulse response more typically seen in an area susceptible to frequent drying and rewetting.

Despite a general understanding of the processes that enable soil moisture to affect Rs, the exact effect of soil moisture is still a subject of debate in literature. Our analysis indicates that soil moisture accounts for approximately 35% of the variability of Rs, and may be more of a control in the early growing season. This is comparable to findings of other studies, that Ts accounts for approximately 60-70% of the variability in Rs while soil moisture is the secondary control (Xu et al., 2004). Further investigation is needed to corroborate this conclusion on the role of soil moisture using longer multi-year observed data time series.

4.2 Spatial variability

The use of automated chambers provides both advantages and disadvantages when dealing with variability in Rs. Automated chamber measurements provide dense temporal resolution, however they capture much less spatial variability as compared to manual Rs measurements. In order to scale Rs from automated chamber-based measurements to annual soil CO_2 fluxes at an ecosystem level, spatial variations in Rs need to be considered (Wang *et al*., 2006). The difference in fluxes measured a meter apart can be as large as differences measured tens of meters apart, even within an area that looks homogenous (Davidson *et al*., 2002). One indicator of the capability of chamber measurements to account for spatial variability is the coefficient of variation (CV) among automated Rs chambers. The CV at our site was found to 50% in 2015, which is comparable to those found in other Rs studies. For example, a study conducted by Shi & Jin (2016) in temperate forests in northeastern China found within-site variations of Rs were 20 to 52%. Another study by Ngao *et al*. (2012) reported CV of 9 to 62% in a European temperate beech forest.

The spatial variation in Rs and its driving factors are currently under-researched due to methodological limitations and its complex origins (Shi & Jin, 2006); however the high CV values obtained in this study as well as previously reported literature indicate that spatial variability is important and should be of concern. Sources of spatial variation in

Rs are reported as largely due to variability of soil organic matter content, root distribution, and soil moisture (Luan et al., 2014; Shin & Jin, 2016).

In order to assess the ability of automated chambers, this study utilized manual chamber measurements conducted at two separate, 50m transects for comparison purposes. Using a combination of both measurement systems provides insight into the spatial representativeness of the automated chamber measurements (Savage & Davidson, 2003), as the larger number of manual collars permit greater spatial distribution. The two systems produced similar results when compared on manual chamber measurement dates, measuring within one standard deviation of each other 93% of the time. Similar comparison studies also found good agreement between manual and automated Rs measurement systems (Savage & Davidson, 2003; Irvine & Law, 2002). There were differences between the two transects, for example the SM at T2 was on average $0.04 m^3 m^{-3}$ higher than T1 and a 2.0 $\mu mol m^{-2} s^{-1}$ lower mean Rs, capturing the spatial variability in major Rs controls.

Overall our results suggest that both automated and manual chamber measurements are in good agreement, but automated chambers are advantageous for their ability to capture high temporal resolution while still being able to account for spatial variation.

4.3 Modeled Rs

4.3.1 Comparison of model fits

From this analysis, the models that produced the best fit for our site were the monthly Q_{10} model (Rs_MQ$_{10}$) and the Q_{10} model with a SM function (Rs_Ts*SM). They both performed better than the simple Rs vs Ts model (Rs_Ts) and conventional annual Q_{10} model (Rs_Q$_{10}$). The short-term (i.e. monthly, daily) temperature response of Rs has been shown to deviate significantly from that for the annual cycle (Jia *et al*., 2013). The annual Q_{10} model may not reflect the true temperature sensitivity since it can be obscured by other seasonally-varying factors such as root biomass, photosynthesis rates, and litter inputs. (Yuste *et al*., 2004; Gaumont-Guay *et al*., 2006). Our analysis agreed with these conclusions. The monthly Q_{10} model was better able to simulate the complex seasonal pattern of Rs-Ts than the annual Q_{10} model. Calculating on a short-term, monthly timescale removes seasonally confounding effects and allows for a better representation of the temporal sensitivity of Rs to Ts (Jia *et al*., 2013).

The conventional annual Q_{10} model also showed improved performance when soil moisture impacts were incorporated using a logistic soil moisture function. Soil moisture has numerous effects on ecosystem metabolism and growth, and thus is an important factor influencing Rs. Low soil moisture conditions can decrease the temperature sensitivity and lower the overall rate of Rs (Xu & Qi, 2001; Davidson & Janssens, 2006; Van der Molen *et al*., 2011). High soil moisture can limit the diffusion of oxygen to microbial communities for R_H (Pumpanen *et al*., 2008). Including soil moisture into Rs-

Ts models improves predictions of Rs, which is supported by previous studies (Wang *et al*., 2006; Geng *et al*., 2012).

Overall the Rs_Q_{10} and Rs_Ts*SM model provided reasonable fit and improvements on the traditional Q_{10} model, but there was still seasonal bias present in the predicted Rs values. The models all overestimated Rs in the autumn, and underestimated Rs in the summer.

4.3.2 Comparison of chamber Rs values with ecosystem respiration.

In order to calculate growing season CO_2 emissions at the TPD study site, a model had to be implemented since there were large percentages of missing measured data. We calculated growing season total Rs values using all four Rs-Ts models and compared them to ecosystem respiration (RE) measured by the eddy covariance system operating at our site. Automated chamber measurements were not maintained during the winter during our study, and as such predicted emissions for winter were not calculated. Previous studies have reported growing season soil carbon emissions of 800 to 1400 g C m^{-2} in temperate forests (Raich & Schlesinger, 1992; Kishimoto-Mo *et al*., 2015; Keidel *et al.*, 2015; Liu *et al*., 2016). Our simulated growing season Rs values for 2014 and 2015 appear to be within this range, with growing season estimated Rs values from 885 to 1593 g C m^{-2}, respectively. Most studies in literature do not include measurements taken in the winter, as it is thought to be a relatively low percentage of total annual Rs and automated chamber measurements are difficult to maintain in the winter season due to snowfall. Liu *et al* (2015) conducted a study in a temperate coniferous forest and found winter Rs to be approximately 5% of total annual emissions, but other studies report contributions between 10-50% (Schindlbacher *et al*., 2007).

Contributions of Rs to RE has been reported as 60-90% in literature (Davidson *et al*., 2002; Yuste *et al*., 2005; Khomik *et al.*, 2006). In our study, the only estimate of growing season Rs that was able to be compared to RE was by the Rs_MQ$_{10}$ model in 2015 (84% of growing season RE). All other models appeared to overestimate Rs, as the chamber-based estimates yielded significantly higher values than eddy covariance derived RE. Previous studies have reported overestimation of Rs by chamber-based measurements (Koskinen *et al*., 2014; Speckman *et al*., 2014). Some possible explanations of this phenomenon may be differences in the spatial coverages of the automatic chamber systems and the eddy covariance flux footprint (Davidson *et al*., 2002; Davidson *et al*., 1998). Though improvements were made, all Rs-Ts models displayed seasonal biases with an underestimation of Rs in the summer and an overestimation in the autumn (Figures 11 and 12). Methodological errors in chamber-based flux measurements have also been proposed as possible sources of overestimation by chamber measurements, such as the disturbance of the soil CO_2 gradient caused by the chamber closing too quickly (Davidson *et al*., 1998; Koskinen *et al.*, 2014). Comparing both study years, the absence of the first half of the growing season in 2014 have also lead to estimation errors.

This study has provided important insight on the temporal and spatial dynamics of Rs. The addition of temporal and SM considerations have been shown to increase the modeling accuracy of the traditional Q$_{10}$ model. Many future climate change scenarios predict an increased probability of intense precipitation events (IPCC, 2014), and a quantitative understanding of the Rs rain response is a necessary consideration in the development of an accurate global carbon cycle model. Future work could include a quantification of the contribution of PPT-induced pulses in Rs to annual total Rs in temperate deciduous forests, as well as the further development of an accurate, predictive model through an improved understanding of the spatial and temporal dynamics of Rs.

5. CONCLUSIONS

In this study, the growing season dynamics of Rs in a temperate deciduous forest was studied using automated and manual chamber measurement systems over a two year period (2014 to 2015). Through the comparison of automated and manual chamber measurements performed along two separate transects, the automated chamber measurements were found to be able to account for spatial variability in Rs within the forest site. Our analysis indicated that Ts was a dominant control and explained annual temporal variability in Rs. Soil moisture also exerted a significant control and accounted for approximately 35% of the variability in Rs in 2015. We observed large pulses of Rs following major rainfall events, which increased Rs by as much as 88% during these periods.

The average annual temperature sensitivity (Q_{10} value) of the study site was found to be 2.34, though the Q_{10} showed significant seasonal variation. R_{10} was found to increase with increasing Ts, while Q_{10} decreased. The annual Q_{10} model was improved by the incorporation of temporal variability of Rs (by estimating on a monthly basis) and through the addition of soil moisture controls via a logistic function. The monthly Q_{10} model estimated Rs with the most accuracy, producing R^2 values of 0.76 to 0.77 as compared to 0.20 to 0.69 for the annual Q_{10} model. The application of the monthly Q_{10} model to growing season data indicated that Rs accounts for 84% of the growing season ecosystem respiration measured by the eddy covariance system at our site.

This study provided insight into the dynamics of Rs in temperate deciduous forests, with important implications for the development of vegetation ecosystem models. Our findings highlight the importance of considering temporal variations when modeling Rs, as well as both temperature and soil moisture controls. Our results also suggest that the potential for increased frequency of extreme weather events in the face of climate change could have implications on future Rs emissions.

REFERENCES

Apps, M. J., & Price, D. (2013) *Forest ecosystems, forest management and the global carbon cycle* (Vol. 40). Springer Science & Business Media. (p. 1-16)

ArchMiller, A., Samuelson, L. (2016) Partitioning longleaf pine soil respiration into its heterotrophic and autotrophic components through root exclusion. *Forests,* **7**: 39.

Bond-Lamberty, B., Thomson, A. (2010) Temperature-associated increase in the global soil respiration record. *Letters to Nature* **464:** 579-583.

Brady, N., Weil, R. (2008) *The Nature and Properties of Soil*. Pearson Education Inc. (p.495-541)

Clemmensen, K., *et al*. (2013) Roots and associated fungi drive long-term carbon sequestration in boreal forest. *Science* **339**: 1615-1618.

Davidson, E., Belk, E., & Boone, R. D. (1998) Soil water content and temperature as independent or confounded factors controlling soil respiration in a temperate mixed hardwood forest. *Glob. Chang. Biol.* **4***:* 217-227.

Davidson, E., Janssens, I. (2006) Temperature sensitivity of soil carbon decomposition and feedbacks to climate change. *Nature* **440**: 165–173.

Davidson, E., Savage, K., Verchot, L., Navarro, R. (2002) Minimizing artifacts and biases in chamber-based measurements of soil respiration. *Agr. Forest Meteorol.* **113**: 21-37.

Davidson, E., Trumbore, S., Amundson, R. (2000) Biogeochemistry: Soil warming and organic carbon content. *Nature* **408**: 789-790.

Don, A., Schumacher, J., Freibauer, A. (2011) Impact of tropical land use change on soil organic carbon stocks – a meta-analysis. *Glob. Chang. Biol.* **17**:1658-1670.

Don, A., Rodenbeck, C., Gleixner, G. (2013) Unexpected control of soil carbon turnover by soil carbon concentration. *Environ. Chem. Lett.* **11**:407-413.

Fontaine, S., Mariotti, A., Abbadie, L. The priming effect of organic matter: a question of microbial competition? *Soil Biol. & Biochem*. **35**: 837-843.

Frey, S., Lee, J., Melillo, J., Six, J. (2013) The temperature response of soil microbial efficiency and its feedback to climate. *Letters to Nature* doi:10.1038/NCLIMATE1796.

Gainey, P. L. (1919) Parallel formation of carbon dioxide, ammonia and nitrate in soil. *Soil Science* **7**: 293-312.

Gaumont-Guay, D., Black, T. A., Griffis, T. J., Barr, A. G., Jassal, R. S., & Nesic, Z. (2006). Interpreting the dependence of soil respiration on soil temperature and water content in a boreal aspen stand. *Agr. Forest Meteorol.* ***140**:* 220-235.

Geng, Y. *et al*. (2012). Soil respiration in Tibetan alpine grasslands: belowground biomass and soil moisture, but not soil temperature, best explain the large-scale patterns. *PloS one* **7:**e34968.

Gonzalez-Benecke, C., Martin, T., Cropper, W., Bracho, R. (2010) Forest management effects on in situ and ex situ slash pine forest carbon balance. *For. Ecol. Manage.* **260**:795-805.

Görres, C., Kammann, C., Ceulemans, R. (2015) Automation of soil flux chamber measurements: potentials and pitfalls. *Biogeosci. Discuss*. **12**: 14693-14738.

Groenigen, K., Xia, J., Osenberg, C., Luo, Y., Hungate, B. (2015) Application of a two-pool model to soil carbon dynamics under elevated CO_2. *Glob. Chang. Biol*. **21**: 4293-4297.

Han, G., Luo, Y., Li, D., Xia, J., Xing, Q., Yu, J. (2014) Ecosystem photosynthesis regulates soil respiration on a diurnal scale with a short-term lag time in a coastal wetland. *Soil Biol. & Biochem*. **68**: 85-94.

Hanson, P., Edwards, N., Garten, C., Andrews, J. (2000) Separating root and soil microbial contributions to soil respiration: A review of methods and observations. *Biogeochem.* **48:** 115-146.

Hogberg, P., *et al.* (2001) Large-scale forest girdling shows that current photosynthesis drives soil respiration. *Nature* **411:** 789-792.

Hogberg, P., *et al.* (2008) High temporal resolution tracing of photosynthate carbon from the tree canopy to forest soil microorganisms. *New Phytol*. **177:** 220-228.

IPCC, 2014: *Climate Change 2014: Mitigation of Climate Change. Contribution of Working Group III to the Fifth Assessment Report of the Intergovernmental Panel on Climate Change* [Edenhofer, O., R. Pichs-Madruga, Y. Sokona, E. Farahani, S. Kadner, K. Seyboth, A. Adler, I. Baum, S. Brunner, P. Eickemeier, B. Kriemann, J. Savolainen, S. Schlömer, C. von Stechow, T. Zwickel and J.C. Minx (eds.)]. Cambridge University Press, Cambridge, United Kingdom and New York, NY, USA.

Irvine, J., Law, B. (2002) Contrasting soil respiration in young and old-growth ponderosa pine forests. *Glob. Chang*. Biol. **8**:1183-1194.

Jacinthe, P., Lal, R. (2006) *Encyclopedia of Soil Science, Volume 2. (p.*1508-1511) Taylor & Francis, New York.

Janssens, I., Kowalska, A., Longdoz, B., Ceulemans, R. (2000) Assessing forest soil CO_2 efflux: an in situ comparison of four techniques. *Tree Physiol.* **(20)**, 23-32.

Janssens, I., Carrara, A., Ceulemans, R. (2004) Annual Q_{10} of soil respiration reflects plant phenological patterns as well as temperature sensitivity. *Glob. Chang. Biol.* **10:** 161-169.

Janzen, H. H. (2004) Carbon cycling in earth systems—a soil science perspective. *Agric. Ecosyst. Environ.* **104:** 399-417.

Jia, X., Zha, T., Wu, B., Zhang, Y., Chen, W., Wang, X., He, G. (2013) Temperature response of soil respiration in a Chinese pine plantation: Hysteresis and season vs. diel Q_{10}. *PLoS ONE* **8:** e57858.

Keidel, L., Kammann, C., Grünhage, L., Moser, G., & Müller, C. (2015) Positive feedback of elevated CO_2 on soil respiration in late autumn and winter. *Biogeosci.* **12:** 1257-1269.

Khomik, M., Arain, A., McCaughey, J. (2006) Temporal and spatial variability of soil respiration in a boreal mixedwood forest. *Agric. For. Meteor*. **140**: 244-456.

Khomik, M., Arain, M., Brodeur, J., Peichl, M., Restrepo-Coupe, N., McLaren, J. (2010) Relative contributions of soil, foliar, and woody tissue respiration to total ecosystem respiration in four pine forests of different ages. *J. Geophys. Res.* **115**:G3.

Kishimoto-Mo, A. W., Yonemura, S., Uchida, M., Kondo, M., Murayama, S., Koizumi, H. (2015) Contribution of soil moisture to seasonal and annual variations of soil CO_2 efflux in a humid cool-temperate oak-birch forest in central Japan. *Ecol. Res.* ***30:*** 311-325.

Koskinen, M., Minkkinen, K., Ojanen, P., Kämäräinen, M., Laurila, T., Lohila, A. (2014) Measurements of CO_2 exchange with an automated chamber system throughout the year: challenges in measuring night-time respiration on porous peat soil. *Biogeosci.* **11:** 347-363.

Kutsch, W. L., Bahn, M. , Heinemeyer, A. (2010) *Soil Carbon Dynamics: An Integrated Methodology.* Cambridge University Press. (p.16-18)

Kuzyakov, Y., Larionova, A (2005) Root and rhizomicrobial respiration: a review of approaches to estimate respiration by autotrophic and heterotrophic organisms in soil. *J. Plant Nutr. Soil Sci.* **168:** 503-520.

Lee, M. S., Nakane, K., Nakatsubo, T., Mo, W. H., & Koizumi, H. (2002) Effects of rainfall events on soil CO_2 flux in a cool temperate deciduous broad-leaved forest. *Ecol. Res.*, **17:** 401-409.

Lee, X., Wu, H. J., Sigler, J., Oishi, C., & Siccama, T. (2004) Rapid and transient response of soil respiration to rain. *Glob. Chang. Biol.* **10:** 1017-1026.

Levy-Varon, J., Schuster, W., Griffin, K. (2012) The autotrophic contribution to soil respiration in a northern temperate deciduous forest and its response to stand disturbance. *Oecologia* **169**: 211-220.

Liao, C., & Zhuang, Q. (2015) Reduction of Global Plant Production due to Droughts from 2001 to 2010: An Analysis with a Process-Based Global Terrestrial Ecosystem Model. *Earth Interac.* ***19*****:**1-21.

Liu, L., *et al*. (2015) A cross-biome synthesis of soil respiration and its determinants under simulated precipitation changes. *Glob. Chang. Biol.,* **22:** *1394-1405.*

Liu, B., *et al.* (2016) Annual soil CO_2 efflux in a cold temperate forest in northeastern China: effects of winter snowpack and artificial nitrogen deposition. *Sci. Rep. 6.*

Lloyd, F., Taylor, J. (1994) On the temperature dependence of soil respiration. *Funct. Ecol*. **8**: 315-323.

Lorenz, K., Lal, R. (2010) *Carbon sequestrations in forest ecosystems*. Springer Science & Business Media.

Lu, X., Fan, J., Yan, Y., Wang, X. (2013) Responses of soil CO_2 fluxes to short-term experimental warming in alpine steppe ecosystem, northern Tibet. *PLoS ONE* **8:** e59054. Doi:10.1371/journal.pone.0059054.

Luo, Y., Wan, S., Hui, D., Wallace, L. (2001) Acclimatization of soil respiration to warming in a tall grass prairie. *Nature* **413:** 622-625.

Ma, Y., Piao, S., Sun, Z., Lin, X., Wang, T., Yue, C., Yang, Y. (2014). Stand ages regulate the response of soil respiration to temperature in a Larix principis-rupprechtii plantation. *Agric. For. Meteor.* **184:**179-187.

Matsumoto, K., *et al*. (2008) Energy consumption and evapotranspiration at several boreal and temperate forests in the Far East.*Agric. For. Meteorol.* **148**: 1978–1989.

Michael, L., Goulden, J., Munger, W., Fan, S., Daube, B., Wofsy, S. (1996) Measurement of carbon sequestration by long-term eddy covariance: methods and a critical evaluation of accuracy. *Global Change Biol.* **2:**169-182.

Mitra, B., Mackay, D., Pendall, E., Ewers, B., Cleary, M. (2014). Does vegetation structure regulate the spatial structure of soil respiration within a sagebrush steppe ecosystem? *J. Arid Environ.* **103**:1-10.

Moyano, F., Kutxch, W., Rebmann, C. (2008) Soil respiration fluxes in relation to photosynthetic activity in broad-leaf and needle-leaf forest stands. *Agric. For. Meteorol*. **148:**135-143.

Nagy, Z., Pinter, K., Pavelka, M., Darenova, E., Balogh, J. (2011) Carbon fluxes of surface vs. ecosystems: advantages of measuring eddy covariance and soil respiration simultaneously in dry grassland ecosystems. *Biogeosci.* **8:**2523-2534.

Nemani, R., *et al*., (2003) Climate-driven increases in global terrestrial net primary production from 1982 to 1999. *Science*, **300**: 1560–1563.

Ngao, J., Epron, D., Delpierre, N., Bréda, N., Granier, A., Longdoz, B. (2012) Spatial variability of soil CO_2 efflux linked to soil parameters and ecosystem characteristics in a temperate beech forest. *Agric. For. Meteorol*. **154:** 136-146.

Noh, N., Kuribayashi, M., Saitoh, T., Nakaji, T., Nakamura, M., Hiura, T., Muraoka, H. (2015) Responses of soil, heterotrophic and autotrophic respiration to experimental open-field soil warming in a cool-temperate deciduous forest. *Ecosystems*, DOI: 10.1007/s10021-015-9948-8.

Pavelka, M., Sedlak, P., Acosta, M., Czerny, R., Taufarova, K., Janous, D. (2007) Chamber techniques versus eddy covariance method during nighttime measurements. *International Scientific Conference,* September 17-20.

Peichl, M., Arain, M. Brodeur, J. (2010) Relative contributions of soil, foliar, and woody tissue respiration to total ecosystem respiration in four pine forests of different ages. *Agric. For. Meteorol*. **150:** 1090-1101.

Petit, J., *et al.* (1999). Climate and atmospheric history of the past 420,000 years from the Vostok ice core, Antarctica. *Nature*, **339:** 429-436.

Pumpanen, J., *et a*l. (2008) Respiration in boreal forest soils as determined from carbon dioxide concentration profile. *Soil Sci. Soc. Am. J.* **72:** 1187-1196.

Raich, J., Schlesinger, W. (1992) The global carbon-dioxide flux in soil respiration and its relationship to vegetation and climate. *Tellus B.*, **44:** 81-99.

Raich, J., Tufekcioglu, A. (2000) Vegetation and soil respiration: correlations and controls. *Biogeochem.,* **48**: 71-90.

Ryan, M., Law, B. (2005) Interpreting, measuring and modeling soil respiration. *Biogeochem.* **73**: 3-27.

Savage, K., Davidson, E. (2003) A comparison of manual and automated systems for soil CO_2 flux measurements: Trade-offs between spatial and temporal resolution. *J. Exp. Botan.* **54:** 891-899.

Savage, K., Parton, W., Davidson, E., Trumbore, S., Frey, S. (2013) Long-term changes in forest carbon under temperature and nitrogen amendments in a temperate northern hardwood forest. *Glob. Chang Biol.* **19:** 2389-2400.

Schimel, D. (2014) Forests in the Global Carbon Cycle. In *Challenges and Opportunities for the World's Forests in the 21st Century* (pp. 231-239). Springer, Netherlands.

Schindlbacher, A., Zechmeister-Boltenstern, S., Glatzel, G., Jandl, R. (2007) Winter soil respiration from an Austrian mountain forest. *Agric. For. Meteorol*. **146:** 205-215.

Schlesinger, W., Andrews, J. (2000) Soil respiration and the global carbon cycle. *Biogeochem*. **48**: 7-20.

Shabaga, J., Basiliko, N., Caspersen, J., Jones, T. (2015) Seasonal controls on patterns of soil respiration and temperature sensitivity in a northern mixed deciduous forest following partial-harvesting. *For. Ecol. Manag.*, **348** 208-219.

Shi, B., & Jin, G. (2016) Variability of soil respiration at different spatial scales in temperate forests. *Biol. Fertil. Soils* 1-11.

Snell, H., Robinson, D., Midwood, A. (2014). Minimising methodological biases to improve the accuracy of partitioning soil respiration using natural abundance ^{13}C. *Rapid Commun. Mass Spectrom.* ***28:*** 2341-2351.

Speckman, H, Frank, J, Bradford, J., Miles, B., Massman, W., Parton, W., Ryan, M. (2015) Forest ecosystem respiration estimated from eddy covariance and chamber measurements under high turbulence and substantial tree mortality from bark beetles. *Glob.Chang. Biol.* ***21:*** 708-721.

Suseela, V., Conant, R., Wallenstein, M., Dukes, J. (2012) Effects of soil moisture on the temperature sensitivity of heterotrophic respiration vary seasonally in an old-field climate change experiment. *Glob.Chang. Biol.* **18**: 336–348.

Taylor, A., *et al*. (2015). Radiocarbon-Based Partitioning of Soil Respiration in an Old-Growth Coniferous Forest. *Ecosyst.* **18:** 459-470.

Thangarajan, R., Bolan, N., Tian, G., Naivdu, R., Kunhikrishnan, A. (2013) Role of organic amendment application on greenhouse gas emission from soil. *Sci. Total Environ*. **465**: 72-96.

Theenhaus, A., Scheu, S. (1996) The influence of slug (Arion rufus) mucus and cast material addition on microbial biomass, respiration and nutrient cycling in beech leaf litter. *Biol. Fertil. Soils*. **23**: 80-85.

Tomè, E., *et al.*, (2016) Mycorrhizal contribution to soil respiration in an apple orchard. *Appl. Soil Ecol*. **101**: 165-173.

Tucker, C., Bell, J., Pendall, E., Ogle, K. (2012) Does declining carbon-use efficiency explain thermal acclimation of soil respiration with warming? *Glob. Chang. Biol.* Doi:10.1111/gcb.12036.

Van't Hoff, J., (1898) Lectures on theoretical and physical chemistry. In: Lehfeldt, R.A. (Ed.), Chemical Dynamics: Part 1. Edward Arnold, London, UK (translated from German).

Van der Molen, M.K., et al. (2011) Drought and ecosystem carbon cycling. *Agric. For. Meteorol.* **151:** 765-773.

Wang, C., Yang, J., & Zhang, Q. (2006) Soil respiration in six temperate forests in China. *Glob. Chang. Biol.* **12:** 2103-2114.

Wang, B., Zha, T., Jia, X., Wu, B., Zhang, Y., Qin, S. (2014) Soil moisture modifies the response of soil respiration to temperature in a desert shrub ecosystem. *Biogeosci.* **11**:259-268.

Wei, W., Weile, C., Shaopeng, W. (2010) Forest soil respiration and its heterotrophic and autotrophic components: Global patterns and responses to temperature and precipitation. *Soil Biol. Biochem.*, **42:** 1236-1244.

Xu, L., Baldocchi, D., Tang, J. (2004) How soil moisture, rain pulses, and growth alter the response of ecosystem respiration to temperature. *Glob. Biogeochem. Cycles, 18*(4).

Xu, M., Qi, Y. (2001). Soil-surface CO_2 efflux and its spatial and temporal variations in a young ponderosa pine plantation in northern California. *Glob. Chang. Biol.* **7:** 667-677.

Yan, L., Chen, S., Xia, J., Luo, Y. (2014) Precipitation regime shift enhanced the rain pulse effect on soil respiration in a semi-arid steppe. *PloS one*, **9:** e104217.

Yuste, C., Janssens, J., Carrara, A., Ceulemans, R. (2004) Annual Q_{10} of soil respiraction reflects plant phenological patterns as well as temperature sensitivity. *Glob. Chang. Biol*. **10**:81-94.

Yuste, J., Nagy, M., Janssens, I., Carrara, A., Ceulemans, R. (2005) Soil respiration in a mixed temperate forest and its contribution to total ecosystem respiration. *Tree Physiol.* **25**: 609-619.

TABLES

Table 1. The organic compounds in plant tissues, organized into broad classes showing their relative percentage within typical green-plant material and relative rate of decomposition, adapted from The Nature and Properties of Soils (p.488-500) by Brady & Weil, 2008.

Classification	**Composition of plant materials (%)**	**Rate of decomposition**
Sugars and starches	5	Rapid
Crude proteins	8	
Hemicellulose	18	
Cellulose	45	
Fats and waxes	2	
Lignins and phenolic compounds	22	Very slow

Table 2. Selected values of soil nutrient content of the litter fall horizon (LFH), and soil depths of 0-15, and 15-35 cm at the site.

Soil Layer	**OM** (%)	**P** (ppm)	**K** (ppm)	**Mg** (ppm)	**Ca** (ppm)	**pH**	**C/N Ratio**
Litter	28.8	93	127	274.3	2186	6.0	15.9
0-15cm	3.5	126	24	52	458	4.9	13.3
15-35cm	1.3	170	10	33	315	5.3	12.7

Table 3. Monthly averages of air temperature (Ta), soil temperature(Ts) at 5cm depth, soil moisture content (SM) at 5cm depth, photosynthetically active radiation (PAR), and monthly precipitation (PPT) totals over the study period measured by the site weather station.

Month	**Ta** (ºC)		**Ts** (ºC)		**SM** (m^3m^{-3})		**Precipitation** (mm)		**PAR** (µmol $m^2 s^{-1}$)	
	2014	**2015**	**2014**	**2015**	**2014**	**2015**	**2014**	**2015**	**2014**	**2015**
Jan	-7.6	-6.2	0.09	-0.04	0.10	0.09	336	53	110.3	105.5
Feb	-7.2	-11.4	-0.03	-0.34	0.09	0.05	162	13	197.7	201.0
Mar	-3.5	-1.5	-0.04	-0.01	0.10	0.10	75	35	279.9	282.2
Apr	6.7	7.0	3.7	2.5	0.16	0.14	119	77	340.4	328.2
May	13.9	16.1	11.9	12.1	0.14	0.10	98	69	410.9	433.0
Jun	20.2	18.1	16.5	15.4	0.06	0.13	42	155	490.9	416.3
Jul	20.1	21.3	17.8	18.0	0.10	0.10	112	44	461.9	487.9
Aug	20.0	20.4	17.7	18.1	0.10	0.06	40	55	397.6	429.6
Sept	17.2	19.6	16.0	17.2	0.11	0.05	144	63	331.2	327.2
Oct	11.7	11.4	11.5	11.9	0.15	0.08	147	113	174.4	201.3
Nov	3.0	8.3	5.0	8.4	0.15	0.11	106	62	96.3	149.3
Dec	0.8	5.3	3.0	5.8	0.14	0.11	46	70	72.2	59.0

Table 4. Seasonal and growing season totals of ecosystem respiration (RE) and measured soil respiration (Rs) values, in g C m^{-2}, and the percentage of missing Rs measurements during the study period.

Season	**RE** (gCm^{-2})		**Rs Measured** (gCm^{-2})		**Missing Data** (%)	
	2014	**2015**	**2014**	**2015**	**2014**	**2015**
Spring	132 ± 1.6	173 ± 1.7	--	105 ± 0.8	100	57.4
Summer	524 ± 3.6	617 ± 3.5	484 ± 1.5	624 ± 1.6	41.3	3.3
Autumn	279 ± 3.8	259 ± 1.8	316 ± 1.8	247 ± 1.0	0	0
Totals	935 ± 2.3	1049 ± 3.0	800 ±2.5	976±2.2	46.3	17.9

Table 5a. Rs model parameters fitted to daily Rs measurements.

Model Label	**Model Name**	**2014**	**2015**
A	Rs_Ts	$Rs = 1.13e^{0.12Ts}$	$Rs = 1.63e^{0.074Ts}$
B	Rs_Ts*SM	$Rs = 344*2.94^{(\frac{(Ts-10)}{10})}*(\frac{1}{1+EXP(5.17-2.51*SM)})$	$Rs = 344*2.94^{(\frac{(Ts-10)}{10})}*(\frac{1}{1+EXP(5.17-2.51*SM)})$
C	Rs_Q_{10}	$Rs = 3.03*3.92^{((Ts-10)/10)}$	$Rs = 3.53*1.64^{((Ts-10)/10)}$

Table 5b. Rs model parameters fitted to monthly data (Model D, Rs_MQ$_{10}$)*.

		2014		**2015**	
Model D	**Month**	**R$_{10}$**	**Q$_{10}$**	**R$_{10}$**	**Q$_{10}$**
Rs_MQ$_{10}$	Apr	3.03*	3.92*	3.53*	1.64*
	May	3.03*	3.92*	2.07	2.26
	Jun	3.03*	3.92*	3.05	4.97
	Jul	3.30	3.74	8.33	0.86
	Aug	4.05	2.30	5.07	1.13
	Sept	3.14	2.93	4.36	1.11
	Oct	3.41	3.11	3.30	2.89

---

* Denotes period where no monthly Q$_{10}$ parameters were able to be calculated (due to instrument error or outside of the active measurement period). Annual Q~~$_{10}$~~ coefficients were used.

Table 6. Statistics for the applied Rs models. Relative root mean square error (RRMSE), relative bias (RB), coefficient of determination (R^2), root mean square deviation (RMSD).

Label	**Model Name**	**2014**				**2015**			
		RRMSE	**RB**	**R^2**	**RMSD**	**RRMSE**	**RB**	**R^2**	**RMSD**
A	Rs_Ts	24.1	-12.8	0.63	1.50	33.8	-2.7	0.37	1.66
B	Rs_Ts*SM	16.4	4.2	0.74	1.25	31.5	-6.9	0.55	1.41
C	Rs_Q_{10}	19.2	-0.9	0.69	1.35	32.5	5.6	0.20	1.87
D	Rs_MQ_{10}	15.4	3.5	0.77	1.17	18.6	-1.6	0.76	1.01

Table 7. Estimated seasonal and total Rs over the growing season using four Rs models.

Model Name	**Rs_Ts** (g C m^{-2})		**Rs_T*SM** (g C m^{-2})		**Annual Q$_{10}$** (g C m^{-2})		**Monthly Q$_{10}$** (g C m^{-2})	
Season	**2014**	**2015**	**2014**	**2015**	**2014**	**2015**	**2014**	**2015**
Spring	231±1.6	185±1.5	156±1.2	161±1.4	168±1.7	195±1.7	183±1.8	150±1.8
Summer	925±1.4	543±1.3	599±1.4	573±1.6	758±1.5	628±1.0	753±1.5	468±1.4
Autumn	437±1.8	301±2.0	345±1.9	325±1.4	345±2.4	273±2.1	321±1.6	267±1.5
Totals	1593±3.3	1030 ± 1.6	1100±1.2	1059±2.5	1271±3.0	1096±1.0	1256±2.7	885±2.2

FIGURES

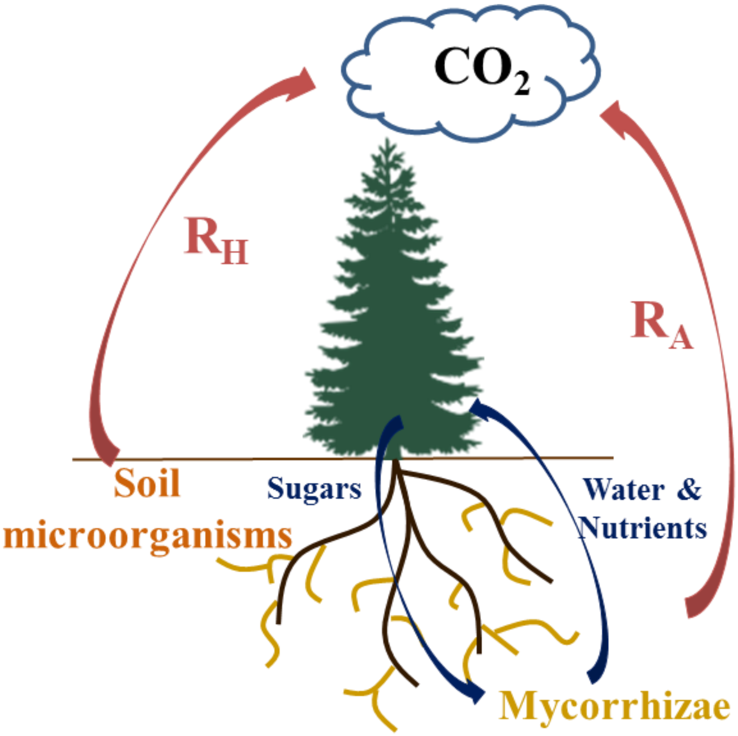

Figure 1. A simplified illustration of the autotrophic (R_A) and heterotrophic (R_H) respiration, including the symbiotic relationship between roots and their associated mycorrhizae.

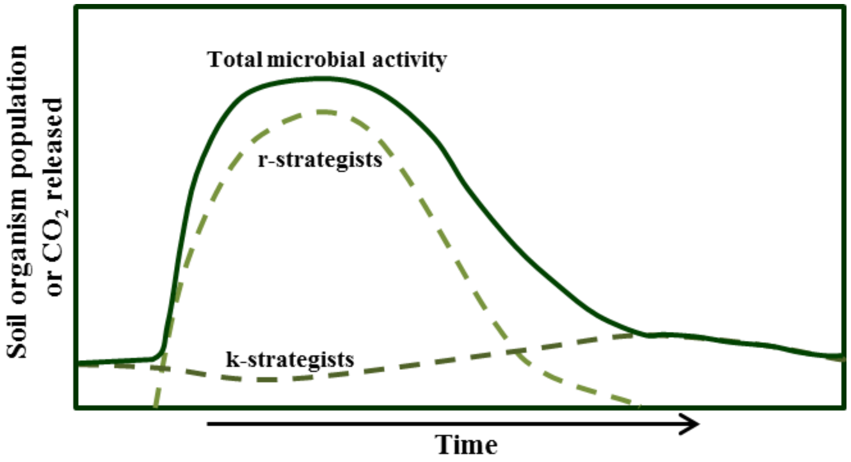

Figure 2. Visualization of the total microbial activity involved in heterotrophic respiration over the growing season, broken down into activity by k-strategists and r-strategist microorganisms. Adapted from *The Nature and Properties of Soils* (p.502) by Brady & Weil, 2008.

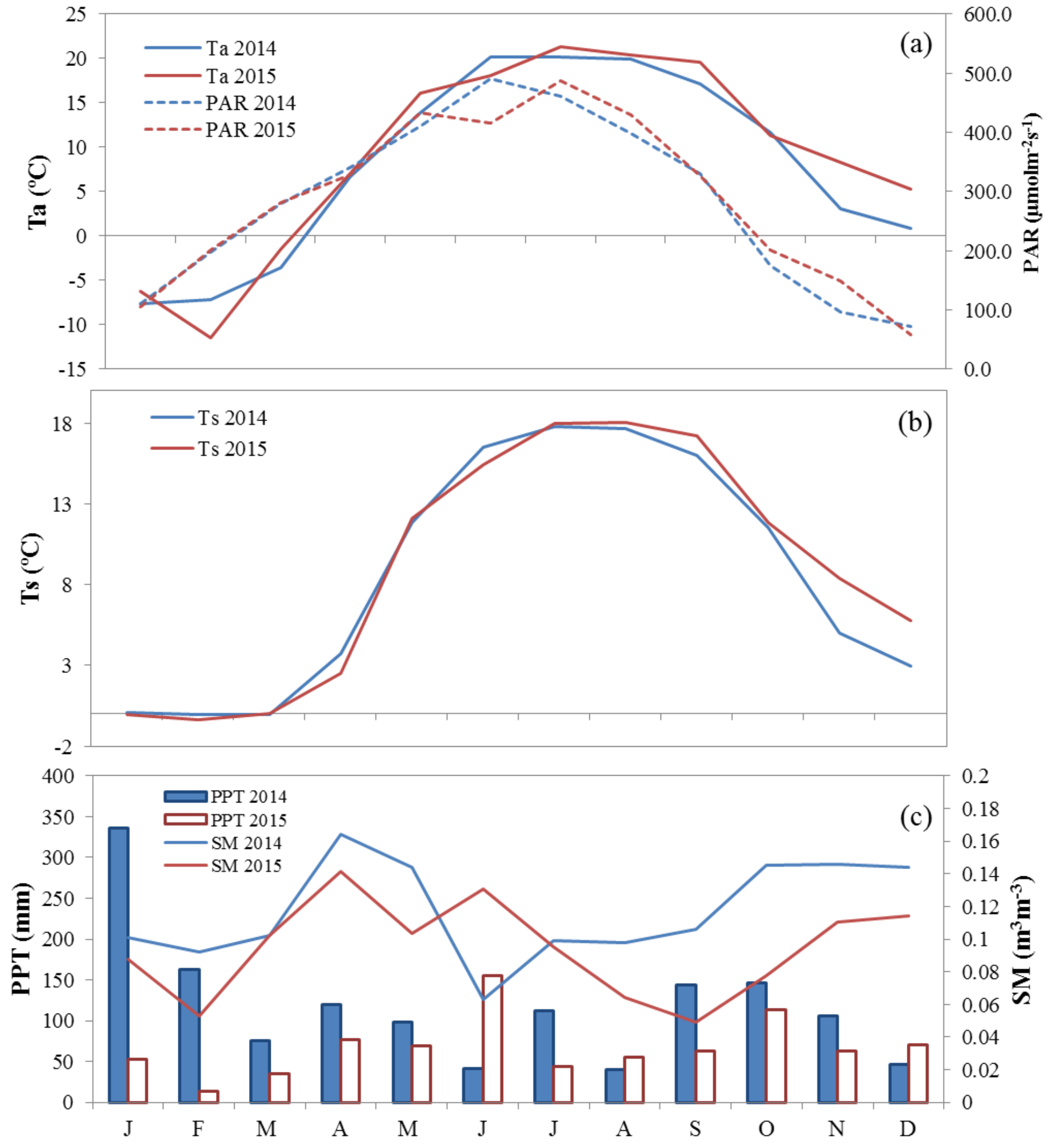

Figure 3. Comparison of climatic conditions during the two year study period (2014 and 2015). (a) Monthly average air temperature (Ta) in ºC and photosynthetically active radiation (PAR) in µmolm^{-2}s^{-1}; (b) monthly average soil temperature (Ts) in ºC; (c) monthly average soil moisture (SM) at 5 cm depth in m^{3}m^{-3} and cumulative monthly precipitation (PPT) in mm. Monthly averages were calculated from half-hourly measurements.

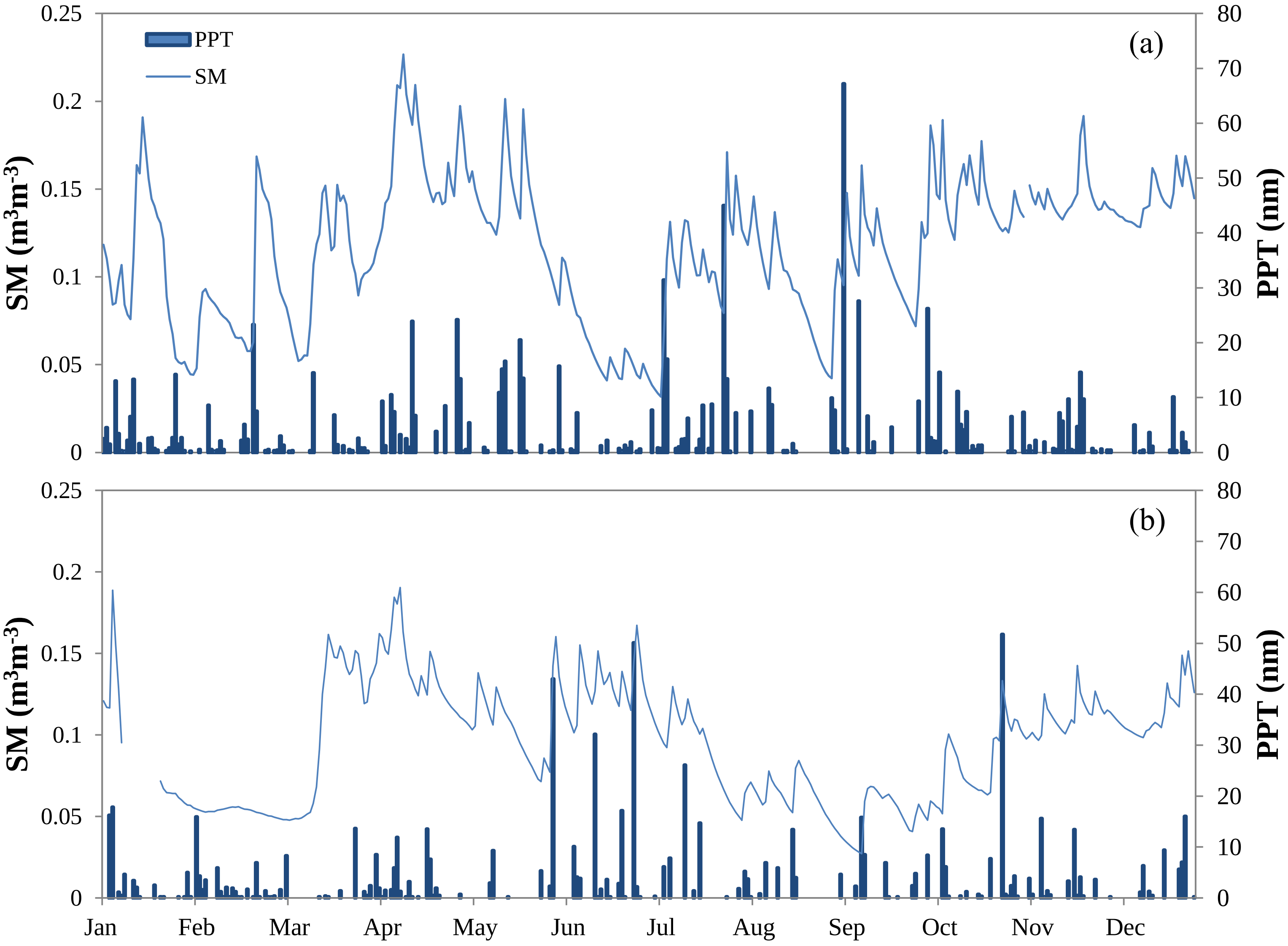

Figure 4. Comparison of daily mean soil moisture content (SM) at 5 cm depth in m^3m^{-3} and cumulative daily average precipitation (PPT) in mm during (a) 2014 and (b) 2015.

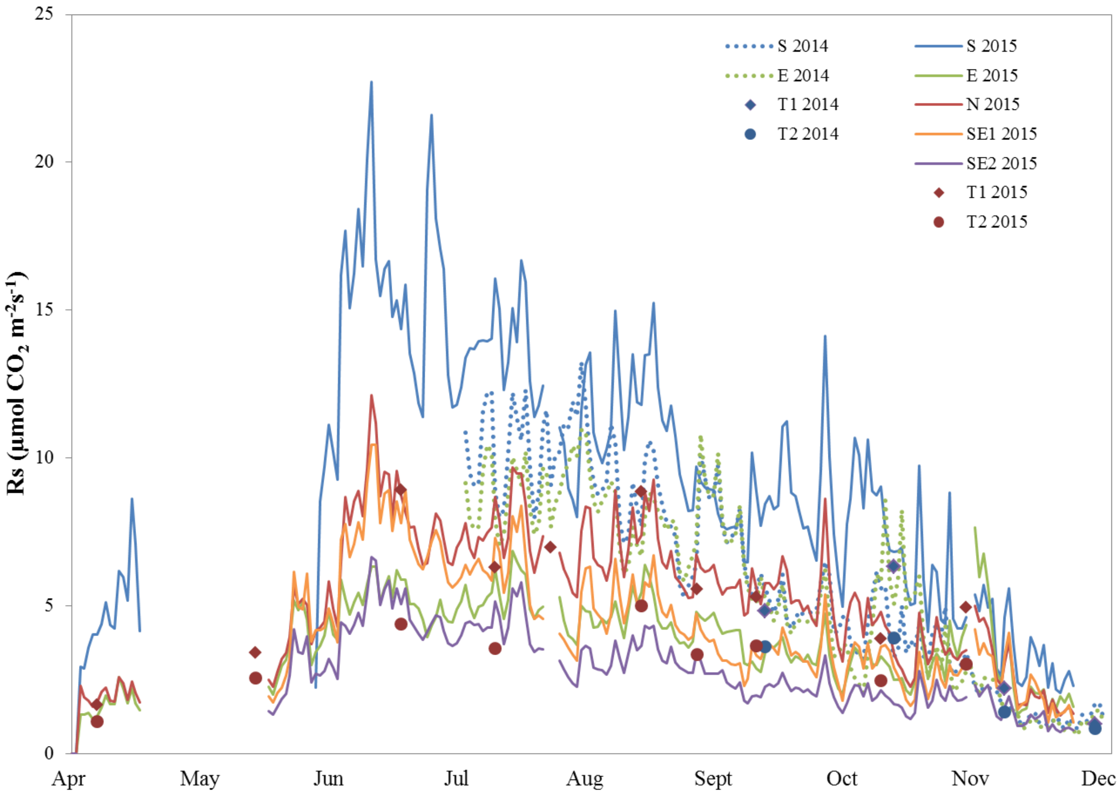

Figure 5. Daily average soil respiration (Rs) in µmol CO_2 m-^{2}s^{-1} measured by automated and manual soil CO_2 chamber systems over the two year study period. Automated chamber measurements are shown for each chamber: South (S), East (E), North (N), Southeast 1(SE1), Southeast 2 (SE2); manual chamber measurements are shown for two 50m transects: Transect 1 (T1) and Transect 2 (T2). Each transect includes ten permanent sampling collars, 5m apart.

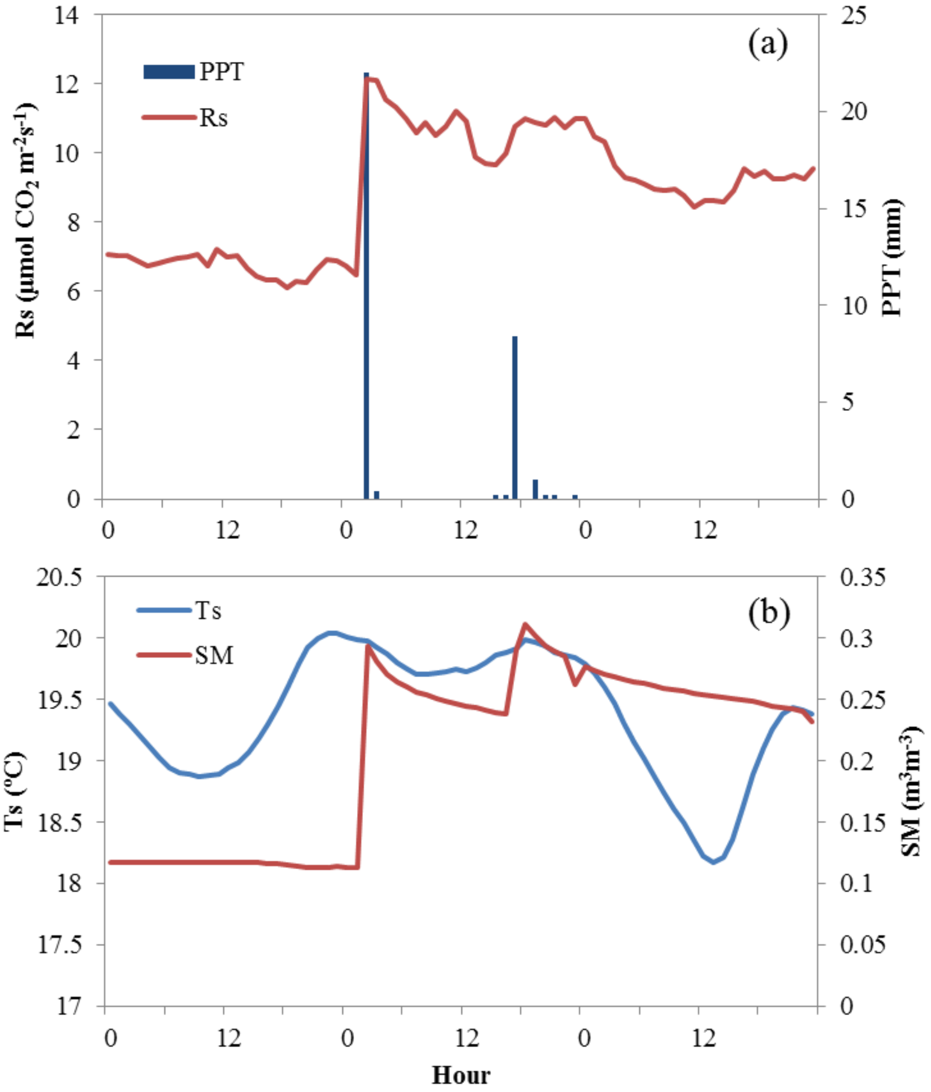

Figure 6. (a) Half hourly soil respiration (Rs) and precipitation (PPT) and (b) half hourly soil temperature (Ts) and soil moisture (SM) at 5 cm depth before, during, and following a 22.4 mm precipitation event on September 2nd, 2014.

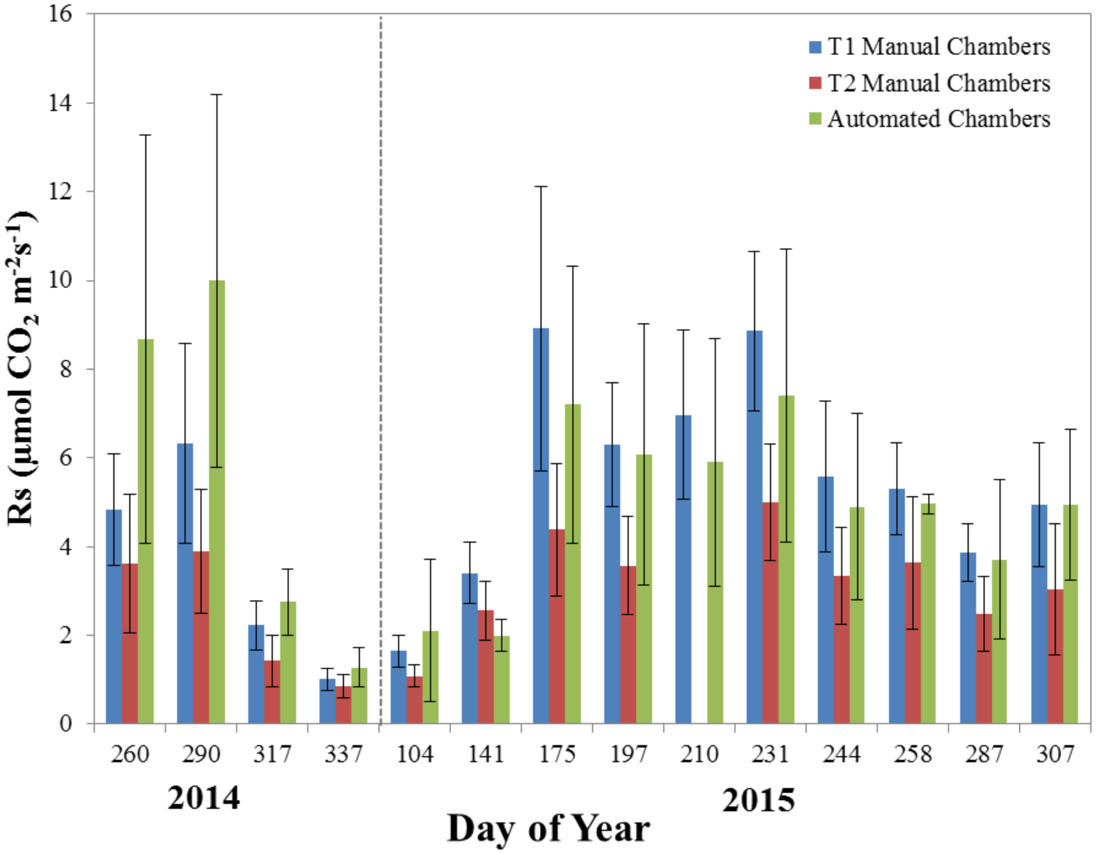

Figure 7. Comparison of the manual soil CO_2 chamber soil respiration (Rs) measurements conducted at Transect 1 (T1) and Transect 2 (T2) against the automated chamber Rs measurements. The error bars indicate standard deviations.

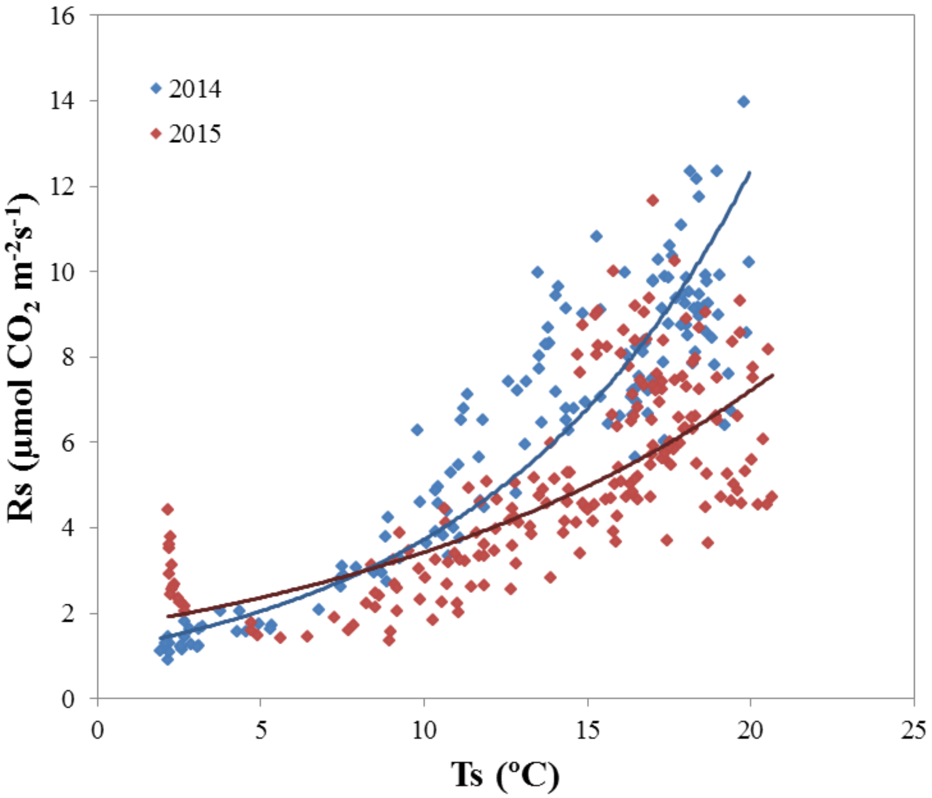

Figure 8. The empirical relationship between daily soil respiration (Rs) in µmol CO_2 $m^{-2}s^{-1}$ and soil temperature (Ts) in ºC measured with the automated chamber temperature probes at 5cm depth during the two year (2014/2015) study period. The fitted Rs_Ts equations and R^2 were found to be $Rs=1.13e^{0.12Ts}$ and 0.63 for 2014 and $Rs=1.63e^{0.074Ts}$ and 0.37 for 2015.

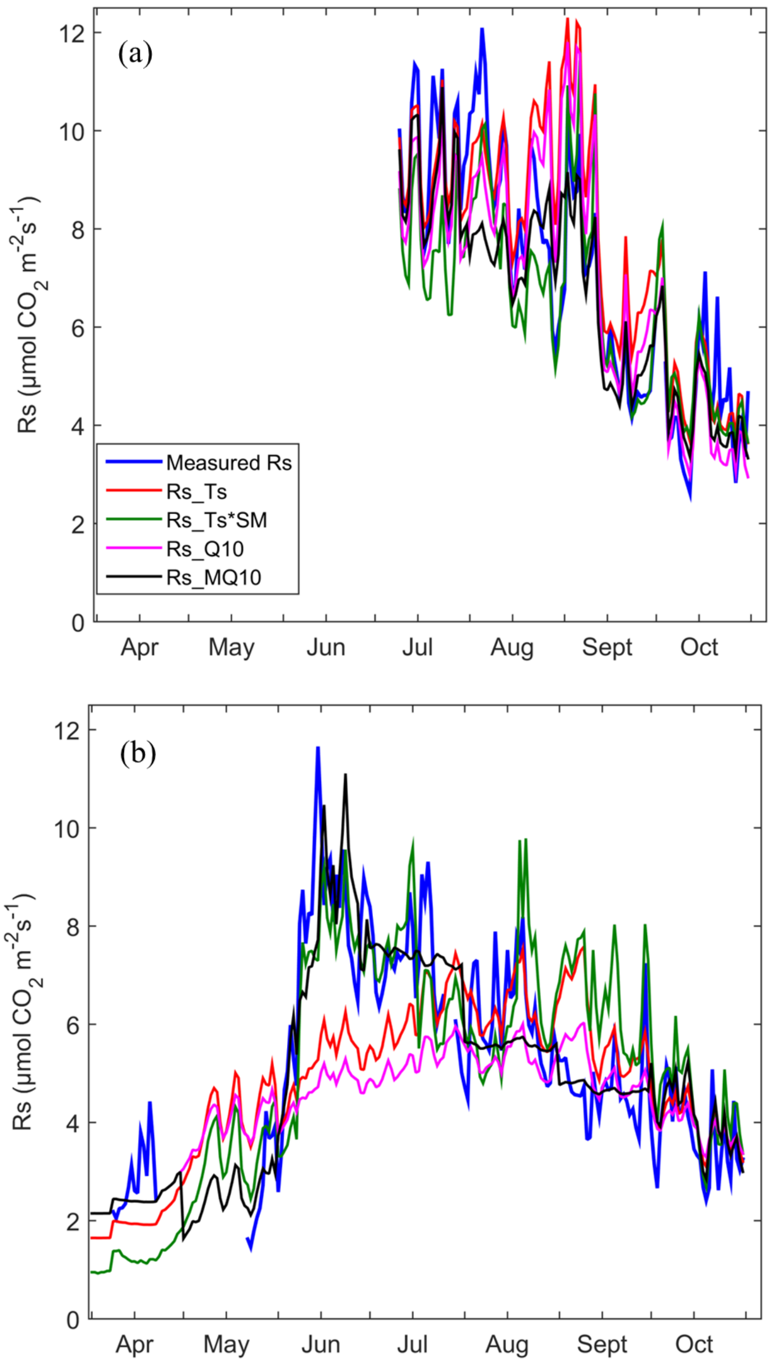

Figure 9. Measured Rs values of daily mean soil respiration during the growing season (April- October) compared with predicted values using four models (Rs_Ts, Rs_Ts*SWC, Rs_Q$_{10}$ and Rs_Q$_{10}$) in 2014 (a) and 2015 (b). Rs is recorded in µmol CO$_2$ m^{-2}s^{-1}

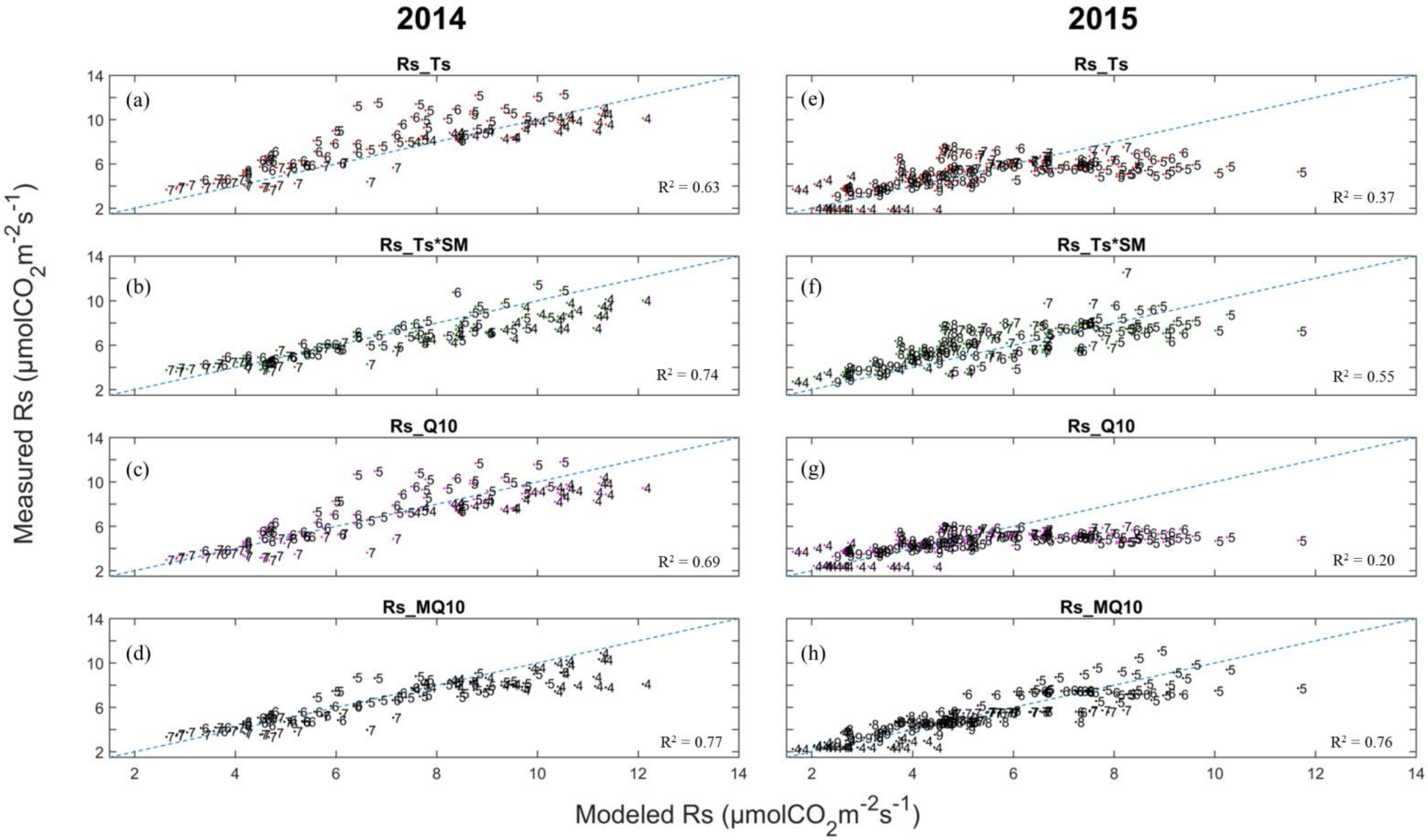

Figure 10. Observed soil respiration (Rs) plotted against modeled Rs and the coefficient of determination (R^2) for each of the four fitted models (Rs_Ts, Rs_Ts*SWC, Rs_Q_{10} and Rs_M Q_{10}) for the growing seasons in 2014 (a, b, c, d) and 2015 (e, f, g, h). The numbers beside data points correspond to the month.

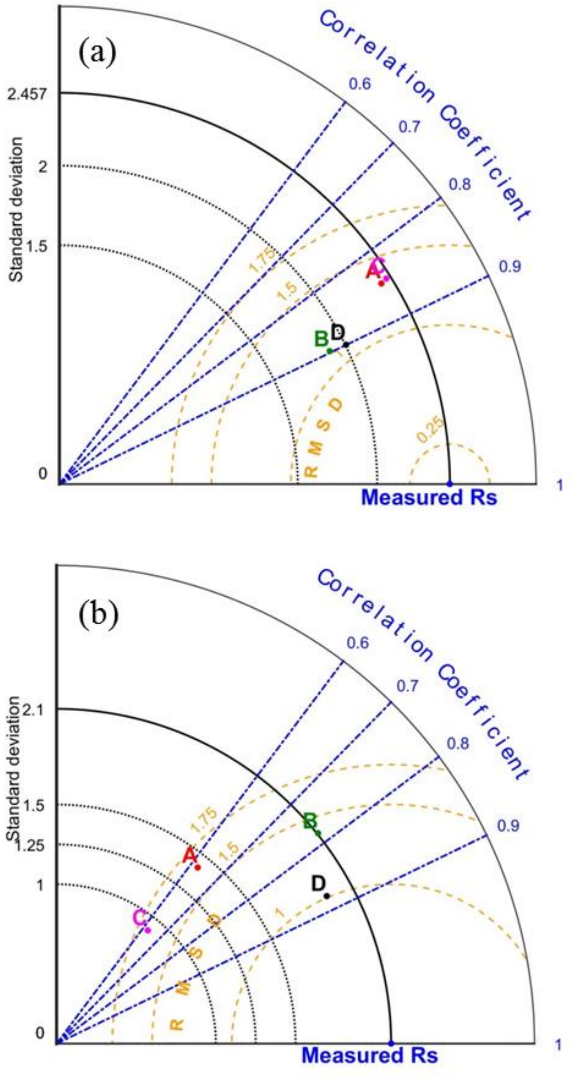

Figure 11. Taylor diagrams comparing model fits in terms of standard deviation, correlation coefficient and root mean square deviation (RMSD) in 2014 (a) and 2015 (b). The models are labelled as (A) Rs_Ts, (B) Rs_Ts*SWC, (C) Rs_Q_{10}, and (D) Rs_MQ_{10}.

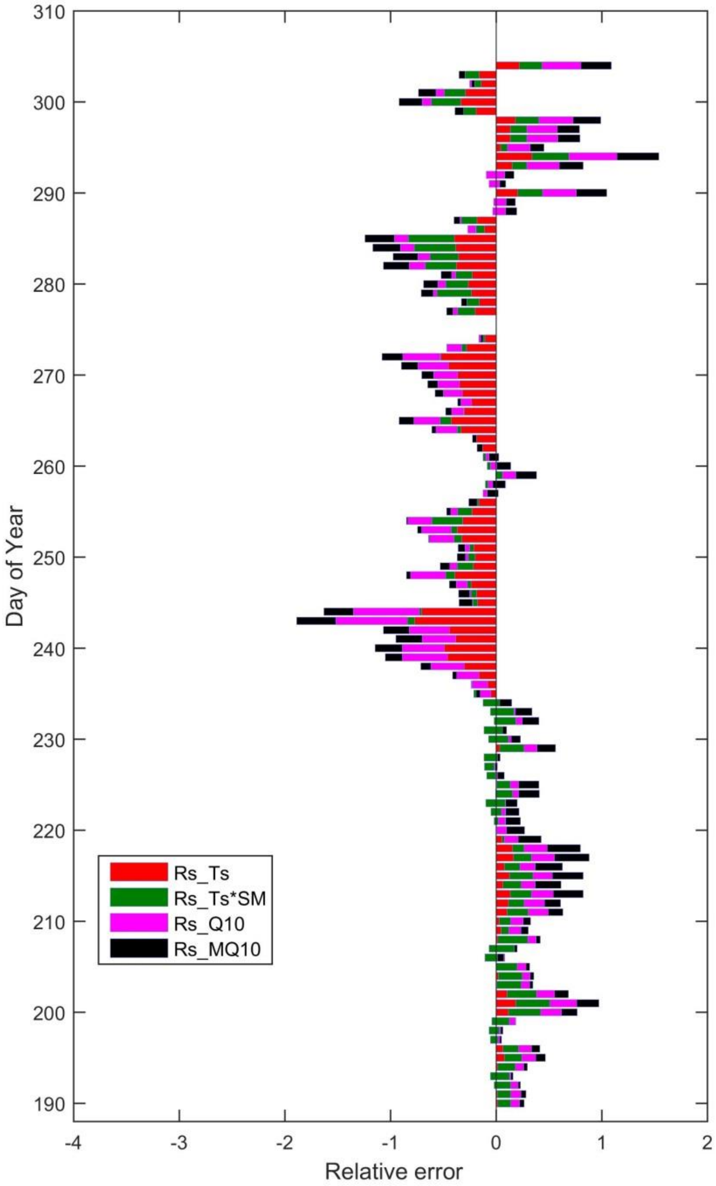

Figure 12. A stacked bar plot showing the daily relative error of each of the four fitted models (Rs_ Ts, Rs_Ts*SWC, Rs_Q_{10} and Rs_M Q_{10}) over the 2014 measurement period (Day of Year 190-339).

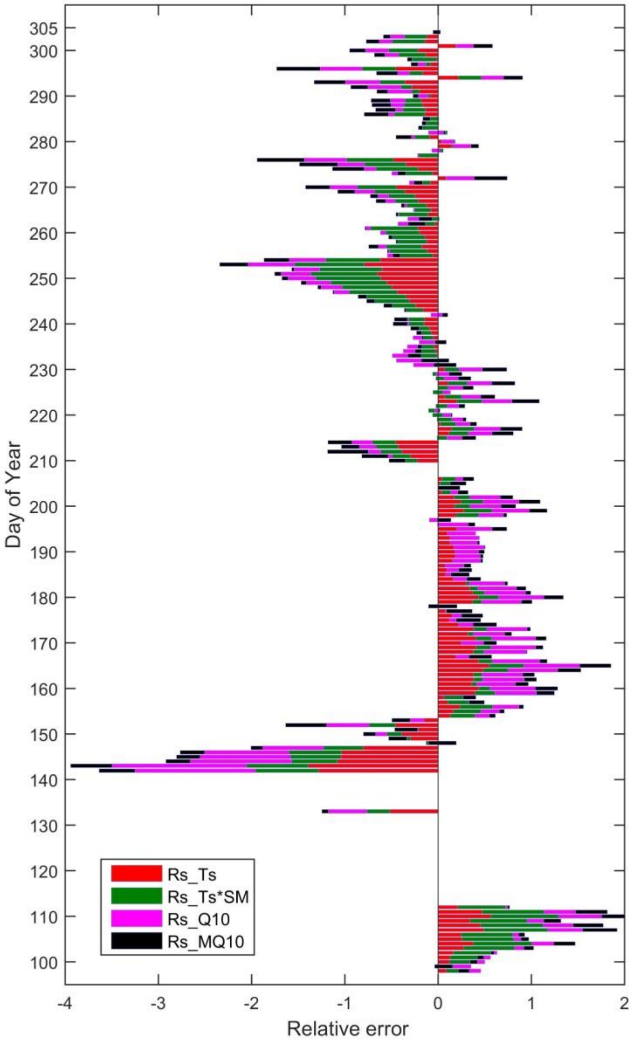

Figure 13. A stacked bar plot showing the daily relative error of each of the four fitted models (Rs_ Ts, Rs_Ts*SWC, Rs_Q_{10} and Rs_M Q_{10}) over the 2015 measurement period (Day of Year 98-330).

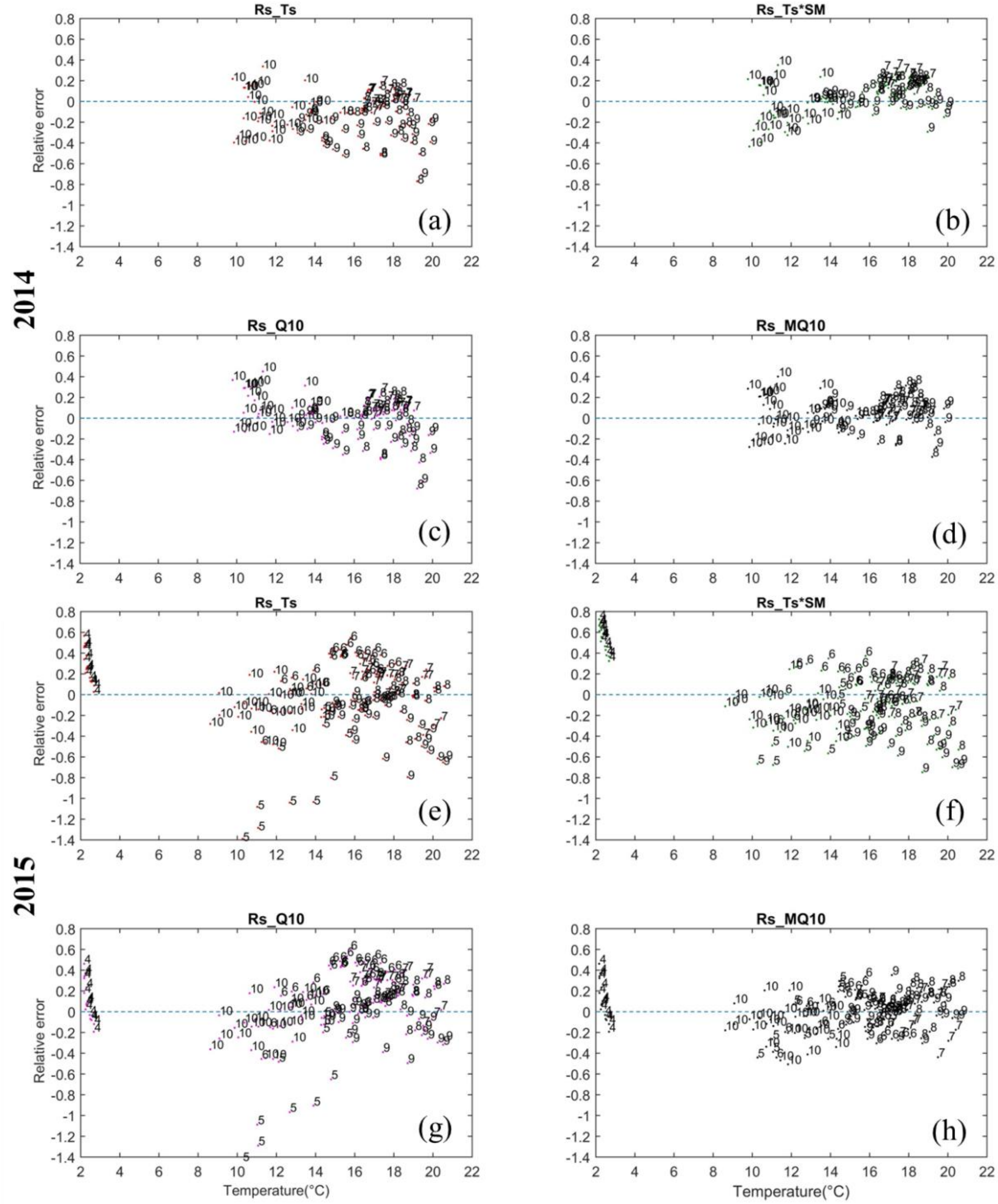

Figure 14. The daily relative error of each of the four fitted models (Rs_Ts, Rs_Ts*SWC, Rs_Q_{10} and Rs_M Q_{10}) plotted against temperature (ºC) for the growing seasons in 2014 (a, b, c, d) and 2015 (e, f, g, h). The numbers beside data points correspond to the month.